NOTE TO USERS

SYNTHESIS AND CHARACTERIZATION OF ELECTROACTIVE POLYMERS AND INTERCALATED NANOCOMPOSITES

A Thesis

Submitted to the Graduate Faculty

in Partial Fulfilment of the Requirements

for the Degree of

Master of Science

in the Department of Chemistry

Faculty of Science

University of Prince Edward Island

Shahidur Rahman Molla

Charlottetown, P. E. I.

August, 2005

Your file Votre référence
ISBN: 0-494-10348-5
Our file Notre référence
ISBN: 0-494-10348-5

SIGNATURE PAGE(S)

Not numbered in thesis

REMOVED

List of Figures

Acknowledgment

Most importantly, I would like to acknowledge Dr. Rabin Bissessur for his thorough guidance, assistance, patience and scholarly knowledge. I pay my thanks to Dr. Kevin Smith for his support. I greatly recognize every help of Dr. Robert Haines.

My gratitude knows no bound when I remember you, Lovely. Without your everyday support, this was impossible. THANK YOU. Thank you, Nelson Zhang, Liping Song for your encouragement, companionship and everything else. I would like to thank Dawna Lund and Sharon Martin for their cordial assistance.

I would like to thank my family, friends, lab mates and above all my parents.

ABSTRACT

The intercalation chemistry of molybdenum trioxide (MoO_3), tin disulfide (SnS_2) and graphite oxide (GO) has been investigated. Poly[oxymethylene-(oxyethylene)] (POMOE) and polyoligo(ethylene glycol) oxalate] (POEGO) have been completely inserted into the layered host of commercially available MoO_3 by exploiting the swelling properties of its lithiated phase. On the other hand, partial intercalation of POMOE and POEGO into lithiated tin disulfide was obtained. The encapsulation of POMOE in the graphite oxide layered system was found to be complete. The new intercalated nanocomposites were characterized by XRD, TGA and elemental analysis.

A simple route for the synthesis of poly[bis-(methoxy ethoxy) phosphazene (MEEP) was developed and the product was characterized by NMR spectroscopy. Poly(dichlorophosphazene) (PDCP) has been synthesized by simple modification of the literature procedure. Synthesis of a new poly phosphazene substituted material was achieved by replacing chlorine atoms from the PDCP backbone with polyaniline. This new material was characterized by NMR spectroscopy.

Glossary of Abbreviations

DCM	Dichloromethane
DMSO	Dimethyl sulfoxide
EM	Emeraldine Base
GO	Graphite Oxide
LLSA	Layer-by-Layer Self-Assembly
LM	Leucoemeraldine Base
MEE	2-(2-methoxy ethoxy) ethanol
MEEP	Poly[bis(2-(2′-methoxyethoxy)ethoxy)phosphazene]
PAH	Poly(allylamine hydrochloride), PAH.
PANI	Polyaniline
PDCP	Poly(dichlorophosphazene)
PDDA	Poly(diallyl dimethyl ammonium) chloride
POEGO	Poly[oligo(ethylene glycol) oxalate)]
POMOE	Poly(oxymethylene oxyethylene)
PSAN	Poly(styrene-co-acrylonitrile)
THF	Tetrahydrofuran

Chapter 1: Introduction

1.1. Intercalation

Literally, intercalation refers to the act of inserting into a calendar some extra interval of time, for example, inclusion of February 29 in a leap year[1]. Today, chemists describe it to be the encapsulation of mobile guest species such as atoms, molecules or ions into crystalline lattices (2D or 3D frameworks) containing interconnected systems of empty sites (□).

$$x\ \text{guest} + \square_x[\text{host}] \rightleftharpoons [\text{guest}]_x[\text{host}] \qquad (1.1)$$

Usually, the process is reversible and topotactic i.e. the structural integrity of the host lattice is maintained in the course of the intercalation (forward) and de-intercalation (backward) reactions. In principle, intercalation reactions can lead to materials with enhanced electrical properties, increased mechanical strength and thermal stability. These enhanced properties are synergistically derived from the two components, which are intimately mixed at the molecular level. This feature makes the study of intercalation chemistry exciting, since there is a wide range of latitude available for controlling many desirable properties in designing materials.

The hosts could be insulators, such as molybdenum (IV) oxide, clays or zeolites, semiconductors *e.g.* transition metal dichalcogenides, or conductors ($LiNi_5$). Some of the transition metal dichalcogenides, such as niobium diselenide ($NiSe_2$) are metallic and even superconductors. Encapsulation of guest species can change the conductive properties of the materials. For instance, insertion of hydrogen or alkali metals into some insulator layered host

material such as WO_3 results in a gradual change in electrical properties to semiconducting and to conducting. Some intercalates such as Li/NbS_2 can go from insulating to conducting (NbS_2) by a de-intercalation process.

1.2. Methods of Intercalation

There are five main methods for the preparation of intercalation compounds. These are redox, coordination, acid-base, ion-exchange and exfoliation/restacking.

1.2.1. Redox Type

Inclusion of alkali metal ions into certain lamellar hosts can be achieved by chemical or electrochemical techniques. Chemical intercalation occurs when the host material is in contact with an active organoalkali metal compound such as n-butyllithium[2]. The reaction proceeds according to equation 1.2,

$$xC_4H_9Li + MX \rightleftharpoons Li_xMX + {}^{x}/_{2}\, C_8H_{18} \qquad (1.2)$$

Commonly, M = transition metal and X = O, S, Se.

The concentration of the ionic guest species (Li^+) can be tailored by controlling the degree of reduction of the layered host.

1.2.2. Coordination Type

The ability of certain organic guest species to covalently bond to certain inorganic layered hosts attracted the attention of researchers in the early 1980's. Johnson *et al.*[3] reported on the intercalation of pyridine and 4,4/ -bipyridine into

layered molybdenum trioxide where the electron rich nitrogen atoms are directly coordinated to the molybdenum centers.

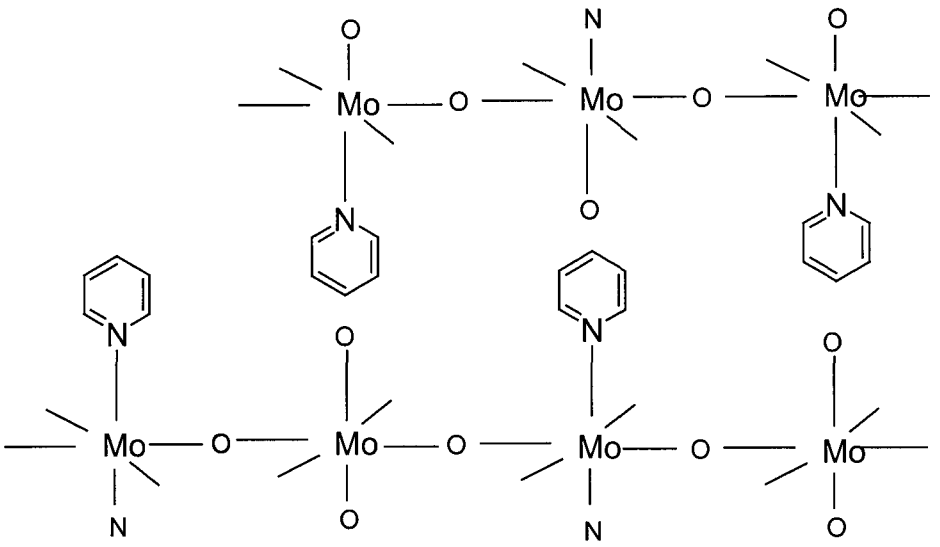

Figure 1.1. Bilayer arrangement of the pyridine guest. The pyridine molecules are covalently bonded to the molybdenums (non-topotactic)[3].

The reaction is non-topotactic, meaning that the structural integrity of the host (MoO_3) is not maintained after inclusion of pyridine.

1.2.3. Acid-Base Type

Intercalation of basic species such as amines into layered acidic hosts has been reported in the literature. Primary n-alkylamine ($C_3H_7NH_2$) can be included into the interlayer gap of vanadyl (IV) hydrogen phosphate hemihydrate ($VOPO_4.0.5H_2O$) to give $VOHPO_4.\ 0.5H_2O.xC_3H_7NH_2$ nanocomposites[4]. The amines insert as bilayers as shown in the Figure 1.2.

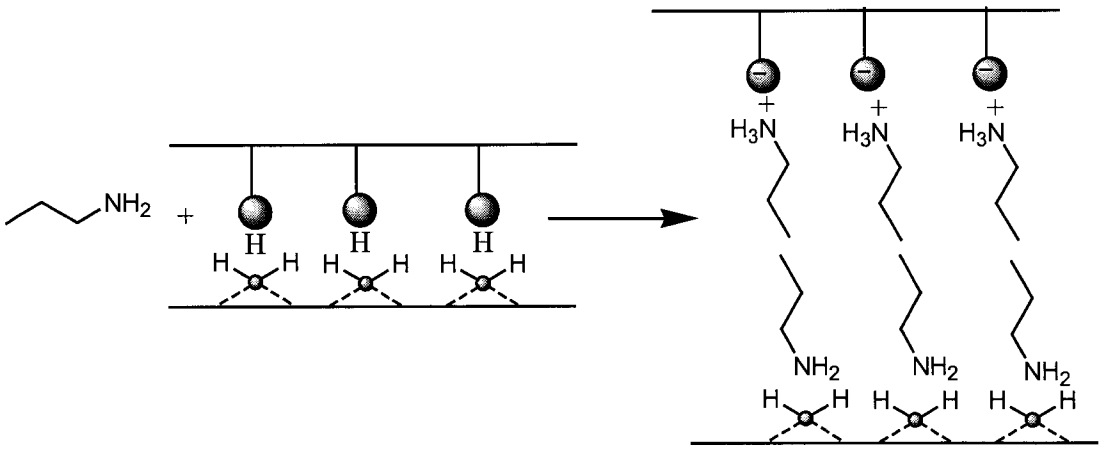

Figure 1.2. Bilayer arrangement of $C_3H_7NH_2$ in $VOHPO_4.0.5H_2O$[4]

1.2.4. Ion-Exchange Type

This is the most common method used in the synthesis of intercalation compounds, where a guest species, G is inserted into the layered host by replacing previously intercalated ions, $G^/$ where $G \neq G^/$. An organophilic clay can be produced from a lamellar structured hydrophilic clay by ion exchange with an organic cation according to the following scheme[5].

$$\text{Na+-CLAY} + \text{HOOC-R-NH}_3^+\text{Cl}^- \rightleftharpoons \text{HOOC-R-NH}_3^+\text{-CLAY} + \text{NaCl} \quad (1.3)$$

1.2.5. Exfoliation/Restacking Type

During the last few decades, the field of intercalation chemistry has been further expanded by the exfoliation-restacking strategy. This method is not limited by the size of the guest species, which could be small molecules[6], cluster compounds[7] or polymers[8,9].

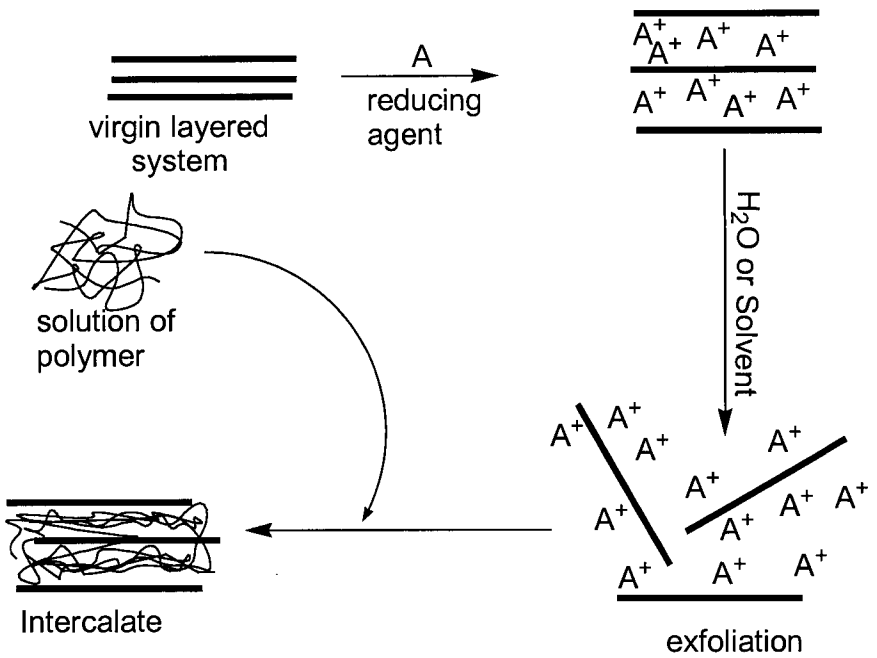

Figure 1.3. Exfoliation-restacking strategy for incorporation of a guest in a layered host

This method has been used to intercalate new materials with specific properties. For example, pyrene and 8-aniline-1-naphthalene sulfonic acid (ANS) have recently been intercalated into MoS_2 by using the exfoliation/restacking properties of $LiMoS_2$[10]. Poly[bis(methoxyethoxy) phosphazene], MEEP[8] and tetraazamacrocycles[11,12] have also been intercalated into molybdenum disulfide.

1.3. Electroactive Polymers

In general, polymeric materials[13] fall into two groups according to the nature of their electric transport – (a) ionically conductive polymers or simply, polymer ionics and (b) electrically conductive polymers or simply called conductive polymers.

1.3.1. Ionically Conductive Polymers

An ionically conductive polymer is a solid polar macromolecule that can act as a solvent for a wide range of salts. The first polymer ionic described in the early 1970's is the complex of poly(ethylene oxide) with alkali metal salts[14]. Ionic conductivity (σ) of an electrolyte system can be expressed as

$$\sigma = nZe\,\mu \qquad (1.4)$$

where n is the number of charge carriers per unit volume, Ze is their charge expressed as a multiple of the charge on an electron, and μ is their mobility, the drift velocity per unit electric field[15]. Higher conductivity can be achieved by increasing the concentration of ionic charge carriers and their mobility.

Conductivities of polymer ionics are restricted by their crystallinity. In fully crystalline materials, the atoms are arranged in a completely ordered pattern. In contrast, atoms in amorphous materials are randomly distributed. Practically, electroactive polymers are semi-crystalline substances consisting of atoms with regular arrangement sites (crystalline zones) and irregular distribution areas (amorphous zones)[16] as illustrated in Figure 1.4.

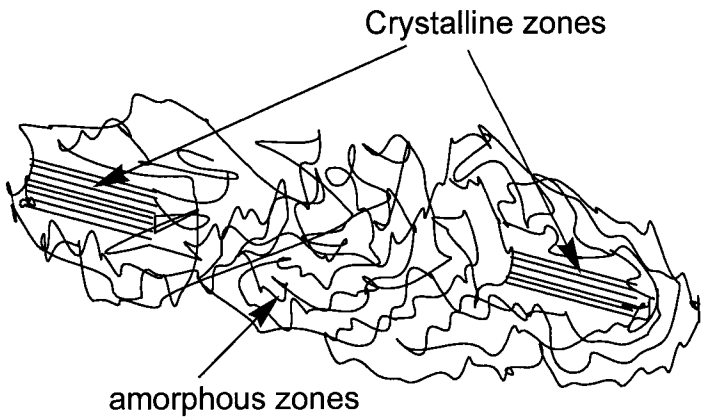

Figure 1.4. Typical semi-crystalline polymer chains consisting of amorphous and crystalline zones

In practice, with change of temperature, crystalline segments within a semi-crystalline polymer melt or freeze at a sharp point, whereas the amorphous regions pass through a glass-transition temperature, (T_g) below which the long chain segment motion is prevented and the chains freeze but become disordered. On the other hand, above T_g, the amorphous segments of the polymers gain vibrational energy that pushes the neighborhood atoms or molecules apart creating *free spaces* or *volumes* and providing flexibility of the polymer. Meanwhile, a number of sophisticated polyethers with reduced crystallinity have been developed at the laboratory level. These include crosslinked (ladder type) and non-crosslinked (comb type).

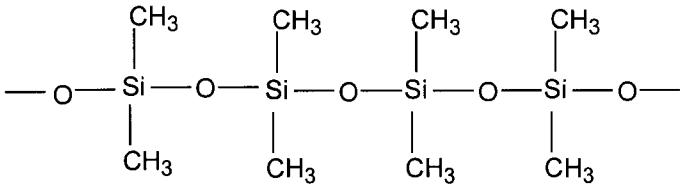

(a) Comb-type polymer

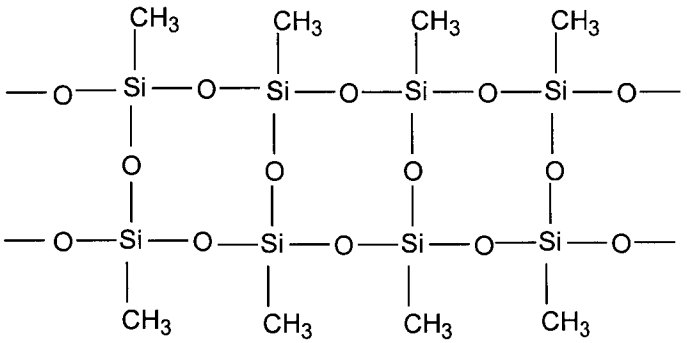

(b) Ladder-type polymer

Figure 1.5. Non-crosslinked (comb-type) and crosslinked (ladder-type) polymers

The next major problem of polymer ionics is their poor mechanical properties. Different strategies have been used to solve this problem. For instance, Toyota Researchers have synthesized nylon-6/clay hybrid materials with enhanced mechanical and thermal properties[17].

1.3.2. Electrically Conductive Polymers

The second group of electroactive polymers as mentioned in section 1.3 is electrically conductive polymers or simply conductive polymers. These are conjugated polymers with modified electronic structures. The processes

to achieve such structures involve p-doping (removal of electron) or n-doping (addition of electron) in the polymer chains.

Nobel laureate Hideki Shirakawa[18] showed the oxidation of polyacetylene, $(CH)_n$ with oxidizing agents such as halogens (p-doping, Equation 1.7) and reduction by reducing agents such as the alkali metal, sodium (n-doping, Equation 1.8).

$$(CH)_n + {}^3/_2 x I_2 \longrightarrow (CH)_n^{x+} + x\, I_3^- \qquad (1.7)$$

$$(CH)_n + x\, Na \longrightarrow (CH)_n^{x-} + x\, Na^+ \qquad (1.8)$$

Polyaniline (PANI) is a very popular conductive polymer.

1.4. Molybdenum trioxide Host System

Molybdenum trioxide, MoO_3 has a layered structure with orthorhombic unit cell of size a = 3.9628 ± 0.0007Å, b = 13.855 ± 0.003Å and c = 3.6964 ± 0.0006 Å [22]. The crystal consists of two-dimensional layered sheets in which MoO_6 octahedra share edges and corners forming a bilayer arrangement in the ac-plane. These sheets of MoO_6 octahedra are held together along the b-direction by van der Waals forces[19] and can be intercalated by simple species such as hydrogen, alkali and alkaline earth metal ions, as well as macromolecules[20].

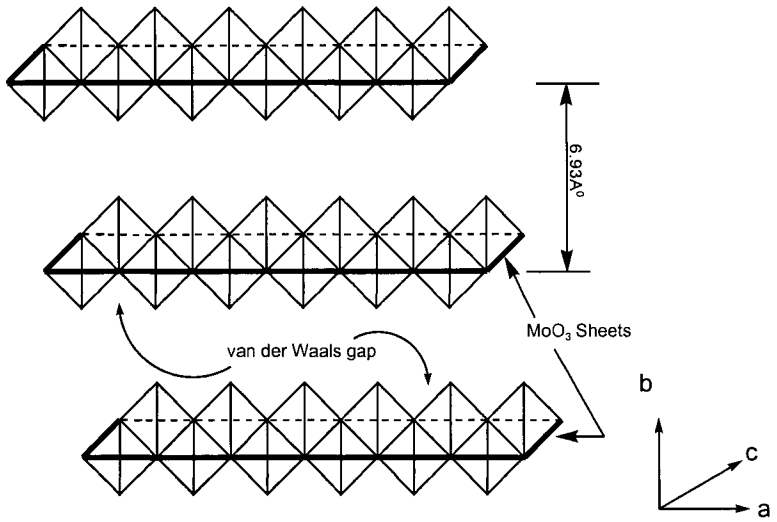

Figure 1.6. Structure of molybdenum trioxide[17]

Some of the well-defined phases of molybdenum oxides reported in the literature include: Mo_4O_{11}[21], $Mo_{17}O_{47}$[22], Mo_5O_{14}[22], Mo_8O_{23}[23], $Mo_{18}O_{52}$[22], $Mo_{19}O_{55}$[24], $Mo_{20}O_{58}$[24], $Mo_{21}O_{61}$[24] and $Mo_{22}O_{64}$[24].

1.4.1. Intercalation of Hydrogen in MoO_3

The inclusion of hydrogen within finely powdered MoO_3 coated with supported catalysts such as platinum at elevated temperatures led to the formation of H_xMoO_3 bronzes ($0.5 \leq x \leq 2.0$)[20]. The hydrogen atoms in the H_xMoO_3 phase are located in the internal spaces of MoO_3 and the phase does not hydrate spontaneously. However, H_xMoO_3 behaves like a Brönsted acid in aqueous metal hydroxide solutions, $A^{z+}(OH^-)_x$, according to Equation 1.9.

$$H_x^+[MoO_3]^{x-} + A^{z+} + mOH^- + nH_2O \rightleftharpoons A_x^{z+}(H_2O)_y[MoO_3]^{x-} \qquad (1.9)$$

Hydrogen bronzes, H_xMoO_3 can also react with Lewis bases (L) such as ammonia, hydrazine, organic amines and heterocyclic bases according to Equation 1.10.

$$Li_xMoO_3 + yL \rightleftharpoons L_{y-y'}H_{x-x'}MoO_3 + y'L + x'Li^+ \qquad (1.10)$$

1.4.2. Intercalatlon of alkaline metals in MoO_3

A hydrated metallic phase, $A_x^+(H_2O)_y[MoO_3]^{x-}$, ($A^+$ = main group or transition metal ion) can be obtained by chemical reduction of MoO_3 with an aqueous solution of a reducing agent.[25] First, a reducing agent such as $NaBH_4$ forms a metal MoO_3 bronze according to Equation 1.11, from which a host of nanocomposites can be obtained by exchanging the sodium ions for other cations.

$$MoO_3 + xNaBH_4 \rightleftharpoons Na_x^+[MoO_3]^{x-} \qquad (1.11)$$

$$Na_x^+[MoO_3]^{x-} + xA^+ \rightleftharpoons A_x^+[MoO_3]^{x-} \qquad (1.12)$$

where, A^+ = alkali/alkali metal ions and organic cations

Hideyuki Tagaya *et al.*[26] showed the formation of a host of nanocomposities by exchanging sodium ions for organic cations. For example, intercalation of anilinium ions in MoO_3 could be achieved by reaction of wet $Na^+_xMoO_3^{x-}$ with anilinium hydrochloride.

Inclusion of polymers into the lamellar structure of MoO_3 has been reported in the past, namely, polymeric ionomer[27,28] such as poly(ethylene

oxide), PEO[29,30], poly(ethylene glycol)[31], poly(propylene glycol)[31], poly(vinyl pyrrolidinone)[31] and methyl cellulose[3].

1.4.3. *In situ* intercalation route to construct polymer/MoO_3 layered structure

Intercalation of conducting polymers such as polyaniline into layered MoO_3 can be done by inserting the monomer molecules (aniline) in MoO_3 and then treating the intercalate (aniline in MoO_3) with an external oxidizing agent such as ammonium peroxydisulfate, $(NH_4)_2S_2O_8$[9].

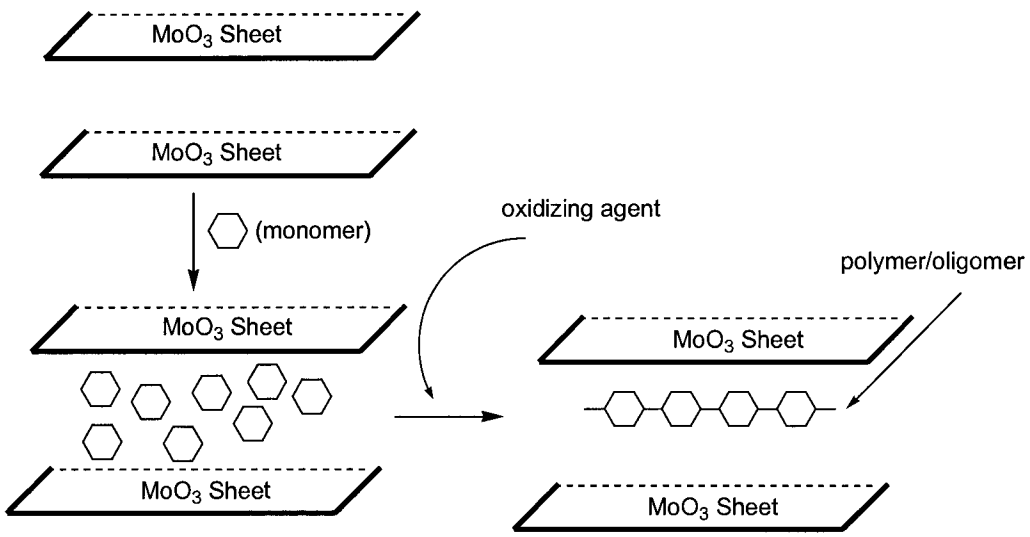

Figure 1.7. In situ intercalation of polymers (polyaniline) in MoO_3

1.5. Tin Disulfide Host System

One of the important characteristics of lamellar chalcogenides is their ability to intercalate guest species in the empty spaces between adjacent chalcogenide sheets, which are bonded by weak van der Waals forces.

Most of the intercalation chemistry has been focused on transition metal chalcogenides as layered hosts with guest species ranging from strong reactants such as hydrazine and alkali metals, to organometallic compounds as well as organic Lewis bases. On the other hand, a very few studies on lamellar chalcogenides of non-transition metal host species have been reported. The prototypical family of such materials is $SnCh_2$ (Ch = S, Se).

Tin disulfide, SnS_2 is an inorganic compound with a hexagonal primitive unit cell, in which the tin atoms are located in octahedral interstices between two hexagonally closed packed slabs of sulfur to form a three-atom layered sandwich. A series of tin-sulfur species are known. These include SnS_2, Sn_2S_3, Sn_3S_4, Sn_4S_5, SnS, and a host of polysulfide anions. The most important prototypes are SnS and SnS_2, both of which are semiconductors with band gaps of 1.3 and 1.8 eV, respectively[32,33]. They can be used as photovoltaic materials[34], and as heat mirrors in solar control coatings[35]. Tin disulfide has useful thermal and hydrolytic stability, low cost and low toxicity compared to other layered dichalcogenides[36].

Many promising new discoveries for both electrodes in solid-state batteries have been developed in the last few decades. Anode materials that have been studied in the past are primarily based on main group metals that include aluminum, silicon, germanium, lead, antimony, bismuth and tin, which react with a lithium to form lithiated alloy[37].

We have chosen SnS_2 as a layered host material to investigate its intercalation behavior with polar polymers such as POMOE and POEGO.

Tin disulfide is commercially available and is an environmentally safe material. However, its intercalation chemistry has not been studied in depth previously.

1.5.1. Intercalation of Lithium in SnS_2

Encapsulation of lithium ions into the van der Waals gap of SnS_2 can be achieved by treatment with an excess amount of n-BuLi in pentane/hexane at room temperature.

$$SnS_2 + C_4H_9Li \xrightarrow[\text{room temp}]{\text{pentane}} LiSnS_2 + {}^1/_2 C_8H_{18} \qquad (1.13)$$

Following the sonochemical method for the preparation of SnS_2 nanoparticles (size 30 nm), the Mukaibo group in Japan showed that reduction of particle size to nano scale enlarges surface area facilitating the lithium ion diffusion.

1.5.2. intercalation of Organic Lewis Bases in SnS_2

Organic Lewis bases can be inserted into SnS_2. The Morales group[38] has shown the intercalation of single layers of aliphatic diamine molecules into the SnS_2 matrix by heating the powdered form of SnS_2 with n-alkyldiamines such as 1,2 diaminoethane and 1,3 diaminopropane at 180^0C in a glass tube sealed under vacuum.

1.5.3. Intercalation of Cationic Clusters and Organic Polymers in SnS_2

Insertion of cationic clusters and organic polymers in the gallery space of SnS_2 can be done by exploiting the exfoliation/restacking properties of SnS_2. For example, the Ollivier group[39] was able to grow alternating layer-by-layer films of the host species, SnS_2 with polymeric cations such as poly(allylamine hydrochloride).

1.6. Graphite Oxide Host System

Graphite is hydrophobic in nature and does not bear any electrical charge. Thus, different methods have been developed for inclusion of hydrophilic polymers such as PEO. One of the important steps in the preparation of graphite/polymer intercalates is the breaking of large graphite crystals into finely powdered exfoliated stacks of graphene layers by chemical or electrochemical oxidation, where graphite grains are disaggregated to spherical particles (diameter <40nm)[40]. The building blocks of graphite oxide[41] are composed of unoxidized aromatic blocks. These blocks are of different sizes separated from each other by six-membered rings containing double bonds and polar functional groups such as hydroxyl, ether and probably carboxylate groups on the surface of the graphene layers (Figure 1.8).

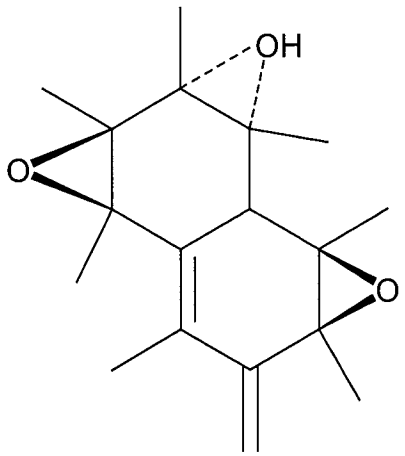

Figure 1.8. A typical structure of graphite oxide[41]

Since graphite oxide has these polar groups, intercalation of polar polymers becomes possible simply by adding GO particles to aqueous solutions of the polymers. Many such intercalation composites have been successfully synthesized including GO/poly(ethylene oxide)[42,43], GO/poly-(vinyl alcohol)[44] and GO/poly(furfuryl)[45].

1.6.1. Intercalatlon of polymers in GO by Exfollation/Restacking Method

The Matsuo group[44] reported the intercalation of PEO (MW, $6*10^6$) into GO. First, GO was suspended in a polar solvent such as water, methanol or ethanol and then PEO dissolved in the same solvent was added to the suspension. As a result, PEO entered in between the exfoliated layered host of

GO and then the layered sheets restacked with the trapped polymer as shown in Figure 1.9.

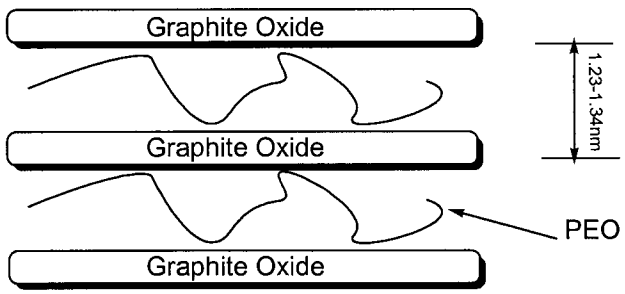

Figure 1.9. Schematic representation of GO/PEO intercalate[43]

The group claimed that exfoliated GO layers were formed by repulsive forces operating between two consecutive GO layers due to the presence of C-O- groups.

1.6.2. Intercalation of polymers in GO by Layer-by-Layer Self-Assembly (LLSA) Method

Multilayer $(GO/PAH)_n$ thin films were prepared by Kovtyukhova *et al.*[43] using the layer-by-layer deposition technique. The multilayered films were grown on one another by alternating adsorption of anionic GO plates and cationic polymers such as poly(allylamine hydrochloride), PAH.

Recently, Dékány and co-workers[40] reported a $(GO/PDDA)_n$ nanocomposite using the LLSA method. In this method, the GO suspension were cast as thin film layers. Since the surface of the sheets was negatively

charged, the deposition of positively charged poly(diallyl dimethyl ammonium) chloride, PDDA became possible (Figure 1.10)

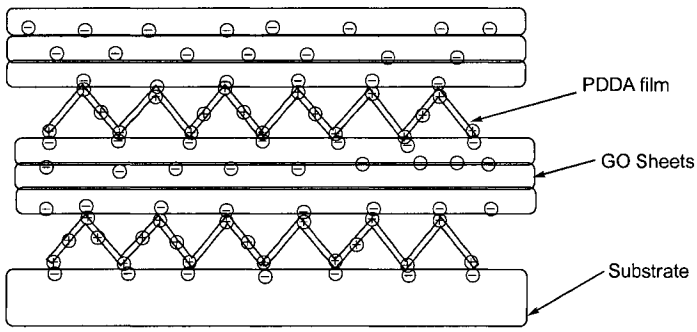

Figure 1.10. Schematic representation of $(PDDA/GO)_n$ films

The assembled GO and PDDA films on a glass substrate are non-conductive and treatment of the films with strong reducing agent, for example hydrazine followed by annealing at high temperature (400^0C) provides granular ordering of the carbon crystallites, which enhances conductivity of the nanocomposite films.

1.6.3. Intercalation of non-polar polymers in GO

In most of the cases, non-polar polymers, including insoluble polymers can not be inserted directly into the GO host. Synthesis GO/non-polar polymer composites can be done by using the *in situ* polymerization process. A noted example is the GO/ PANI intercalated nanocomposite[46].

Exfoliation/adsorption method is usually used to include non-polar materials in GO as shown in Figure 1.11. Exfoliation of GO occurs easily in aqueous alkaline medium. GO is highly porous and can absorb aniline

molecules, which are oxidized to polyaniline using suitable oxidizing agents such as $(NH_4)_2S_2O_8$.

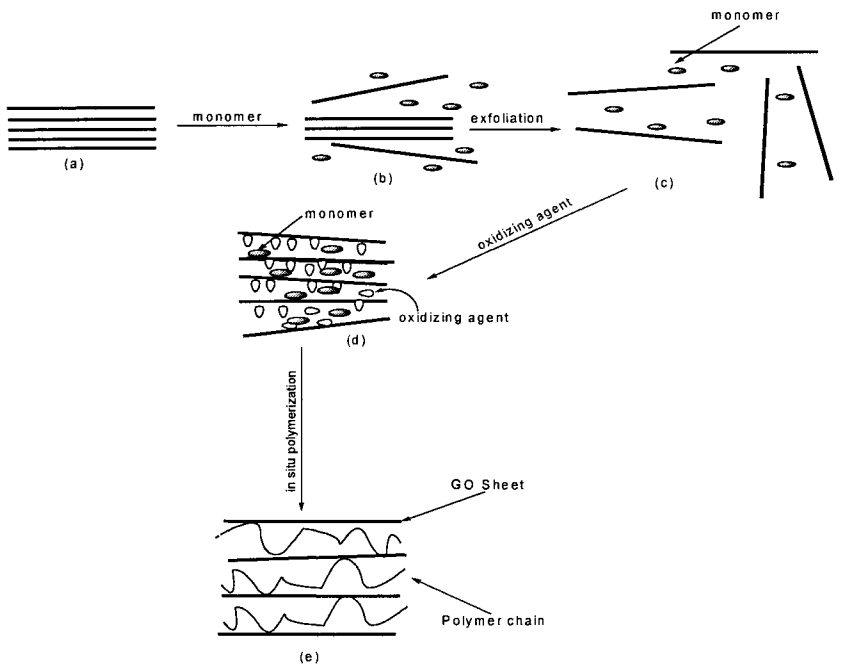

Figure 1.11. Schematic representation for the processing of in situ GO/polymer intercalates: (a) graphite oxide (b) monomer and GO (c) exfoliated GO (d) inclusion of monomers (e) GO/polymer composite

A lightweight and highly conductive GO/poly(styrene-co-acrylonitrile), PSAN composite has been reported by Caiyuan Pan *et al.*[47] The *in situ* polymerization of styrene and acrylonitrile monomers was done into an exfoliated diamond-shaped porous graphite oxide surface at 60-80^{0}C.

1.7. Present Work

The main goal of this project is to synthesize electroactive polymers and intercalate them into different inorganic layered hosts. It has been reported that the movement of ions occurs mainly within the amorphous region of an ionically conducting polymer. Since polyethylene oxide possesses partially amorphous and crystalline segments, several attempts were made to reduce the degree of crystallinity in the polymer matrix. Booth *et al.*[48] synthesized a completely amorphous co-polymer of PEG, namely, poly(oxymethylene oxyethylene), POMOE consisting of -(-CH_2-CH_2-O-)- segments interspersed with –(CH_2-O-)- groups.

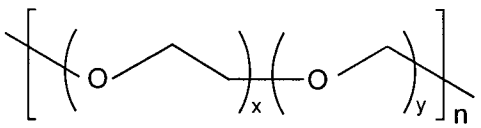

poly(oxymethylene oxyethylene), POMOE

The group showed that a mixture of POMOE and lithium triflate, $LiCF_3SO_3$ ([O]/Li =25) was highly conductive ($3*10^{-5}$ S cm^{-1}) at 25^0C. The Angell group[49] discovered a series of highly conductive ($5.9*10^{-5}$ S cm^{-1}) electrolytes based on poly[oligo(ethylene glycol) oxalate], (POEGO) and lithium salts. The group exploited the idea of Forsyth group, who suggested that introduction of a single carbonate polar group, -[O-C(=O)-O]- into the polyether chain reduces its crystallinity. Interestingly, Angell introduced carbonyl groups in pairs in order to increase the polarity of the polymer matrix.

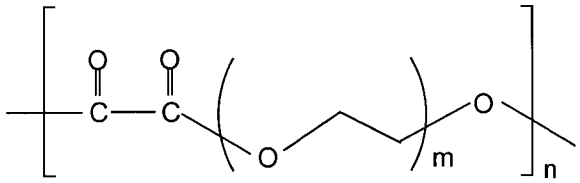

poly(oligo(ethylene glycol) oxalate), POEGO

An increase in polarity means an increase in the dielectric constant of the polymer host and higher dissociation of the dissolved salt or, in other words, higher free ion content of the salt-in-polymer electrolytes. This leads to enhanced conductivity of the material. A lot of work has been reported on the intercalation of PEO into different layered hosts[50-54] while there was no work on the intercalation of amorphous POMOE or POEGO in layered systems until the Bissessur group reported nanocomposite materials of POMOE/MoS_2[9] and POEGO/MoS_2[55] with electronic conductivity of $5*10^{-4}$ S/cm and $3*10^{-1}$ S/cm, respectively.

The current project focuses on the synthesis and characterization of novel intercalated nanocomposite materials of POMOE or POEGO in molybdenum trioxide (MoO_3), tin disulfide (SnS_2) and graphite oxide (GO). This was done by using exfoliation/restacking properties of the layered hosts. The materials were primarily characterized by powder X-Ray diffraction (XRD) and thermogravimetric analysis. POMOE and POEGO have been synthesized according to literature procedures.

In 1984, Allcock and Shriver reported the synthesis of poly[bis(2-(2′-methoxyethoxy)ethoxy)phosphazene] (MEEP), which received considerable

attention because of its molecular flexibility, low glass transition temperature and amorphous nature.

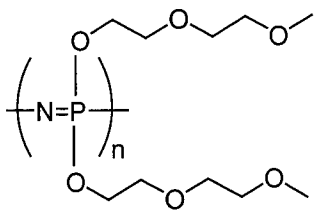

poly[bis(2-(2′-methoxyethoxy)ethoxy)phosphazene] (MEEP)

These properties provide MEEP the capability of solubilizing salts. When complexed with lithium- or silver triflate salts, MEEP displays a room temperature ionic conductivity 2-3 orders of magnitude higher than PEO. The synthesis of MEEP remains a challenge due to the following facts:

(1) ring opening polymerization of the precursor to PDCP always suffers from cross-linking problem, and

(2) the reaction between 2-(2-methoxy ethoxy) ethanol (MEE) and sodium is very slow.

One of the aspects of this project was to overcome these problems. The strategy to achieve this goal is summarized below:

(1) low temperature synthetic method for PDCP (section 2.1.6) avoids the cross-linking problem, and

(2) the use of sodium hydride (section 2.5.3) instead of sodium metal increases the reaction rate for the preparation of the alkoxide solution.

A new PDCP substituted polymer with polyaniline named as Poly[(diPANI)-phosphazene] has been synthesized by replacing the chlorine atoms from the PDCP backbone for PANI.

Chapter 2: Experimental

2.1 Solvent and Reagents

All chemicals used were of analytical grade. Further purification of some of the chemicals was required as described in section 2.2.

Table 2.1. List of the Chemicals Used

Chemical	Source	Purity/Specification
Acetonitrile	Aldrich	HPLC
Ammonium persulfate	Aldrich	99%
Aniline	Aldrich	99%
Benzene	Fisher	98%
Butyllithium	Aldrich	2.5M in hexane
Calcium hydride	Fisher	ACS
Chloroform	Fisher	ACS
Dichloromethane	Caledon	ACS
Dimethyl sulfoxide	Fisher	ACS
Ethanol	Baker	HPLC
Graphite powder	Aldrich	N/A
Hexane	Baker	ACS
Hexatrichlorocyclophosphazene	Aldrich	99%
Hydrazine	Aldrich	99%
Hydrochloric acid	Fisher	ACS
Lithium bis(trimethylsilyl)amide	Aldrich	N/A
Methanol	BDH	ACS

Chemical	Source	Purity/Specification
2-(2-methoxy ethoxy) ethanol	Aldrich	further purified
Molecular Sieve 8-12 mesh	Fisher	pore size 3Å
Molybdenum(IV) oxide	Aldrich	99%
Phosphorus pentachloride	Aldrich	99%
Phosphorus trichloride	Aldrich	2.0M in dichloromethane
Poly ethylene glycol MW 10000	Aldrich	N/A
Poly ethylene glycol MW 100000	Aldrich	N/A
Poly ethylene glycol MW 2000	Aldrich	N/A
Poly ethylene glycol MW 3400	Aldrich	N/A
Poly ethylene glycol MW 400	Aldrich	N/A
Poly ethylene glycol MW 4600	Aldrich	N/A
Poly ethylene glycol MW 8000	Aldrich	N/A
Potassium hydroxide	Fisher	N/A
2-propanol	Aldrich	N/A
Pyridine	Fisher	ACS
Sodium hydride	Fisher	ACS
Sodium hydroxide	Caledon	ACS
Sodium pellet	Aldrich	N/A
Sulfuryl chloride	Aldrich	2.0M in dichloromethane
Sulfuric acid	Aldrich	99%
THF	N/A	N/A
Tin(IV) sulfide	Alfa	99%

CAUTION:

(1) Butyllithium 2.5 M solution in hexane, sodium hydride and lithium bis(trimethylsilyl)amide are explosive and should be kept in the dry box and handled carefully under nitrogen.

(2) Phosphorus trichloride 2.0 M solution in dichloromethane, sulfuryl chloride 2.0 M in dichloromethane and DMSO are toxic and proper safety precautions in handling these compounds is required.

(3) Synthesized PDCP is moisture sensitive and must be handled under nitrogen.

(4) Synthesized $LiMoO_3$ and $LiSnS_2$ may be considered to be explosive and should be kept in the dry box.

2.2. Purification of the Chemicals

Polyethylene glycol, PEG (MW 400) was dried over molecular sieves prior to use. The sieves were heated at 400^0C for four hours and taken quickly into a 250 mL round bottom flask and kept under dry nitrogen flow. After the sieves were cooled down to room temperature, PEG was transferred into the flask by means of a dry syringe and allowed to sit for a few days with occasional agitation to help in the absorption of water molecules.

Dichloromethane, DCM (250mL) was taken into another flask containing an excess amount of CaH_2 and allowed to sit for a few weeks to get rid of moisture. The CH_2Cl_2 was then distilled under nitrogen.

Potassium hydroxide, KOH was used as received from Aldrich. It was then crushed to a fine powder and kept in a desiccator, under vacuum.

Aniline was dried over KOH and distilled under vacuum prior to use and 1M HCL was prepared from 37% HCl.

2.3 Synthesis of Poly[oxymethyleneoxyethylene], POMOE

2.3.1. Procedure

The reaction was carried out in a three neck flask equipped with a dropping funnel containing dry PEG (MW 400) and a mechanical stirrer. The flask was kept under nitrogen flow. Potassium hydroxide (50g, 0.89 mol) and 200 mL of dry DCM was transferred to the three-neck flask. Dry polyethylene glycol MW 400 (50 mL, 0.13 mol) was quickly added to the KOH/DCM slurry from the dropping funnel. The mixture was stirred for 3 days in the dark, at room temperature. The resulting product was air stable, highly viscous and almost colourless. The excess DCM (b.p. 40^0C) was pumped off under reduced pressure. A portion of the product containing excess KOH was then dissolved in deionized water. The solution was transferred to dialysis tubes (molecular weight cut off 3500) and dialyzed till KOH could not be detected as monitored with litmus paper. Finally, the product was then dried under vacuum and freeze-dried till a

clear highly viscous polymer was obtained. The yield of the product was not determined because only a portion of the product was purified.

2.4 Synthesis of Poly[oligo(ethylene glycol) oxalate], POEGO

2.4.1. Chemical Reaction

PEG reacts with oxalic acid dihydrate to produce POEGO (Scheme 2.1)

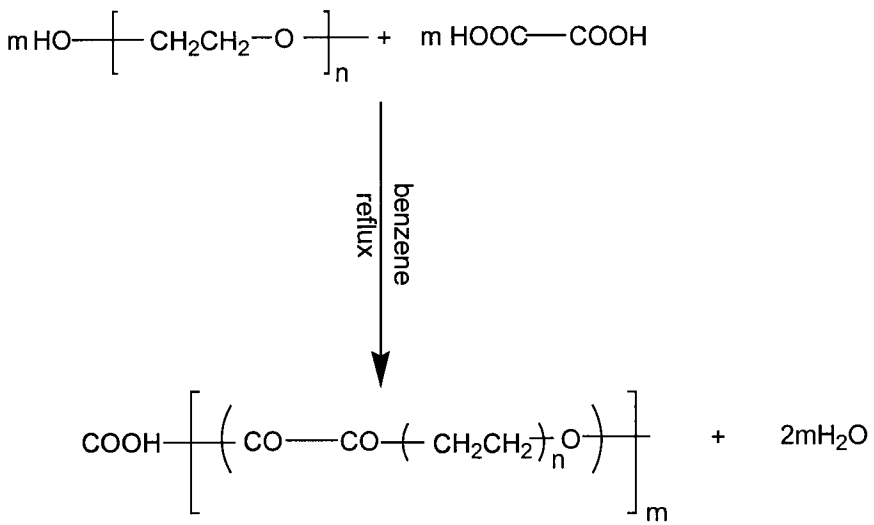

Scheme 2.1. Synthesis of POEGO

2.4.2. Procedure

Poly ethylene glycol MW 400 (5.13g, 0.013 mol) was mixed with oxalic acid (1.62g, 0.013 mol) in a 250 mL round bottom flask. The mass was dissolved in 40 mL of benzene and refluxed in air for 5 days. The excess benzene and water (by product) were pumped off under reduced pressure. After pumping a highly viscous brown liquid material was obtained. The mass was then kept under vacuum overnight. The residual viscous liquid was then heated at 120°C in

a vacuum oven for 2 days. The resulting polymer was highly viscous, slightly hazy and brown in colour. The yield was 4.36 g (84.9%).

2.5 Synthesis of Poly(dichlorophosphazene), PDCP

Poly(dichlorophosphazene) is commercially synthesized by using ring opening polymerization technology (section 2.5.1). Recently, a new low temperature synthetic method for the preparation of PDCP has been developed[58, 59].

2.5.1. Ring Opening Polymerization of PDCP

Stocks[56] reported that heat treatment of hexatrichlorocyclophosphazene (trimer) (Figure 2.2.a) transforms it into a rubbery material, which hydrolyzes to ammonium phosphate and hydrochloric acid.

It took almost 70 years to completely understand the reaction while in 1965, Allcock[57] developed uncross-linked open-chain PDCP at controlled temperature, time, trimer purity and termination of the reaction before 70% conversion of the trimer to the polymer. This linear polymer completely dissolves in organic solvents including tetrahydrofuran (THF), toluene and benzene. Further heat treatment of the species yields cross-linked insoluble rubbery material as described by Stocks.

The findings of Stocks and Allcock are summarized in Scheme 2.2 showing uncontrolled heating of the trimer to form cross-linked PDCP (path a

to c) and controlled experiment as done by Allcock to yield PDCP (path a to b) and cross-linked PDCP (path b to c).

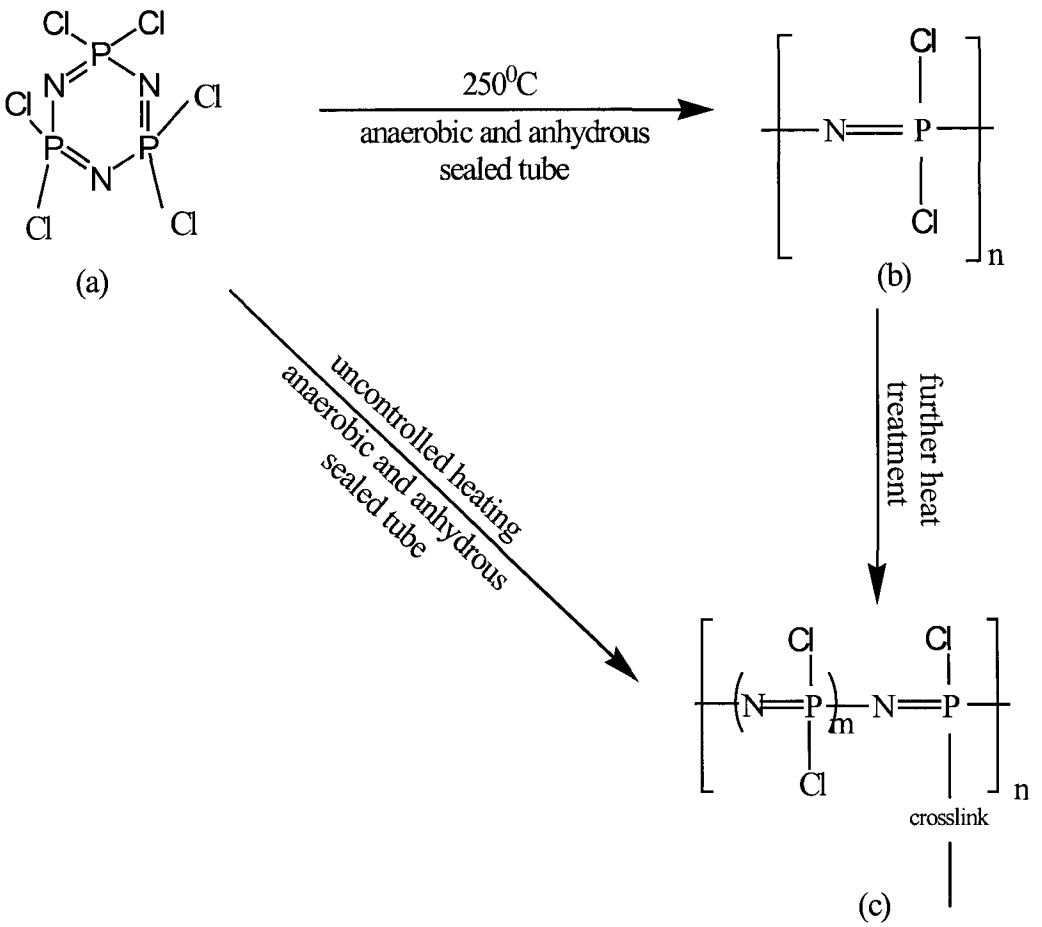

Scheme 2.2. Ring opening polymerizaton of trimer (a) hexatrichloro-cyclophosphazene (b) poly dichlorophosphazene (c) poly cross-linked dichlorophosphazene

However, a certain amount of cross-linking of the PDCP is inevitable during its synthesis when using the ring-opening polymerization technique. To avoid this problem, a low temperature synthesis route has been developed as described in the next section.

2.5.2. Low Temperature Synthetic Method for PDCP

A low temperature synthetic method for the synthesis of PDCP was achieved following the procedure described in the literature[58, 59]. The reaction steps are listed in Scheme 2.3. The experimental procedure has been described in detail under synthesis of MEEP (Section 2.6.1.2.).

$$PCl_3 + Li[N(CH_3)_3Si]_2 \xrightarrow{\text{dry ether}} Cl_2P\text{-}NSi(CH_3)_3 + LiCl \quad (2.1)$$

$$Cl_2P\text{-}NSi(CH_3)_3 + SO_2Cl_2 \xrightarrow{CH_2Cl_2} Cl_3P{=}NSi(CH_3)_3 + SO_2 \quad (2.2)$$

$$Cl_3P{=}NSi(CH_3)_3 \xrightarrow{PCl_5} (NPCl_2)_n \quad (2.3)$$

Scheme 2.3. Low temperature route for the preparation of PDCP[59]

2.6. Modified Route for the Synthesis of MEEP

The synthesis of MEEP involves a three-step process. These steps are - (a) synthesis of PDCP; (b) preparation of an alkoxide solution and (c) refluxing of the PDCP-alkoxide mixture. PDCP was synthesized by using both methods described in section 2.5.

2.6.1.1. Ring Opening Polymerization Method

Five grams of the trimer was transferred into a glass tube that was sealed under vacuum. It was then heated at 250^{0}C for four and a half hours. The

resultant product was a mixture of PDCP, cross-linked PDCP and unreacted trimer. PDCP and cross-linked PDCP were separated from the unreacted hexatrichlorocyclophosphazene by sublimation under vacuum at 40^0C. The yield of PDCP and cross-linked PDCP was 1.32 g (65.7%).

2.6.1.2. Low Temperature Polymerization Method

PDCP was prepared following the literature[58, 59], with some minor modifications. All manipulations for the synthesis of PDCP were carried out under a nitrogen atmosphere. Lithium bis(trimethylsilyl)amide, $LiN[(CH_3)_3Si]_2$ (4.36 g, 0.03 mol) was taken into a round bottom flask from the dry box and placed on an ice bath under a dry nitrogen purge. Approximately 100 mL of dry diethyl ether was poured into another round bottom flask, cooled to 0^0C under nitrogen flow, and nearly 82 mL was transferred to the $LiN[(CH_3)_3Si]_2$. 15 mL (0.03 moles) of 2.0M PCl_3 solution in CH_2Cl_2 kept under nitrogen was added drop by drop for 15 minutes. The reaction mixture was then stirred for an hour at room temperature. The mixture was then cooled down to 0^oC again and 30mL (0.03 moles) of dry 1.0M SO_2Cl_2 in CH_2Cl_2 was added dropwise for 30 minutes using a dry syringe. Stirring was continued for an hour at 0^oC followed by another 45 minutes at room temperature. The resultant mixture was then filtered through a 1 cm layer of celite, which was previously dried in the oven for 5-6 hours under reduced pressure. Two-thirds volume of the volatile materials was pumped off under reduced pressure at room temperature. A very small amount of PCl_5 was then added quickly to the mixture and the mass was stirred overnight at room

temperature. The rest of the volatile materials were removed by pumping and the resultant polymer was freeze-dried for 17 hours. The yield of PDCP was found to be 2.11 g (60.6%).

2.6.2. Preparation of sodium alkoxide solution

The preparation of sodium alkoxide solution was done according to the literature procedure[66]. Seven milliliter (0.06 mol) of dry 2-(2-methoxy ethoxy) ethanol, [$HOCH_2CH_2OC\text{-}H_2CH_2OCH_3$ (MEE)] was taken into a 250 mL round bottom flask and 82 mL of THF from the dry box was added by means of a dry syringe. A slight excess of sodium hydride, NaH (1.6 g, 0.07 mol) was added to the above solution and the reaction mixture was allowed to stir for 4 hours. All the above operations were carried out under dry nitrogen. A light brown solution was obtained.

2.6.3. Refluxing of PDCP- Alkoxide Mixture

In the final step, the sodium alkoxide solution was added to a solution of PDCP (3.42 g, 0.03 mol) in THF (40 mL). The mixture was refluxed and stirred for 24 hours and then all volatile materials were pumped off under reduced pressure. An air stable brown product was obtained. The remaining volatile materials were removed by freeze-drying. Further purification was done by dissolving the materials in deionized water followed by dialysis against water to remove NaCl (by product). After dialysis, the water was removed by freeze-drying. As a result, a very light brown product was

obtained, which was characterized as MEEP (section 3.3). The yield of MEEP was 3.03 g (71.3%),

2.7. Synthesis of Polyaniline (PANI)

Polyanilines are usually represented by the general formula, $[(\text{--B-NH-B-NH-})_y(\text{-B-N=Q=N-})_{1-y})]_x$ where, B is the benzenoid and Q is the quinoid form of the C_6H_4 rings. There are three different oxidation states of polyaniline: (a) fully reduced leucoemeraldine (LM, y = 1), (b) 50% oxidized emeraldine (EM, y = 0.5) and (c) fully oxidized pernigraniline (PAN, y = 0). The polymer can be obtained in its highly conductive state either through the protonation of the imine nitrogens (=N-) in its EM oxidation state, or through the oxidation of the amine nitrogens (-NH-) in its fully reduced LM state[60].

PANI in the following oxidation states were synthesized according to the procedures as reported in the literature[60, 61]. (a) Emeraldine Hydrochloride (~42% Protonation) (b) Conversion of Emeraldine Hydrochloride (~42% Protonation) to the fully protonated (~50%) hydrochloride (c) Synthesis of Emeraldine base, EM and (d) Synthesis of Leucoemeraldine base from EM.

Chemical Reaction

$$C_6H_5NH_2 + (NH_4)_2S_2O_8 \longrightarrow -(C_6H_5NH)-_n + 2H^+ + 2SO_4^{2-} + 2NH_4^+ \quad (2.4)$$

2.7.1 Procedure

The synthesis of Leucoemeraldine base polyaniline involves a four step procedure as described in sections 2.7.1.1 to 2.7.1.4.

2.7.1.1 Synthesis of Emeraldine Hydrochloride (~42% Protonation)

Polyaniline was synthesized by the direct oxidation of aniline using ammonium peroxydisulfate, $(NH_4)_2S_2O_8$, following the procedure reported in the literature[60,61]. Dry aniline (20 mL, 0.5 mol) was dissolved in 300 mL of 1M HCl at 0°C and the solution was stirred in air. Ammonium peroxydisulfate (11.50 g, 0.5 mol) dissolved in 200 mL of pre-chilled 1M HCl was added dropwise with agitation to the above solution. The reactants were allowed to react for 2 hours. As soon as $(NH_4)_2S_2O_8$ was added, the mixture in the reaction flask turned from colourless to blue-green, and became intense blue-green with a coppery glint, with a precipitate forming as the reaction progressed. The precipitate was filtered using a Buchner funnel. The product was then thoroughly washed with precooled 1M HCl and dried overnight under suction. The yield of PANI was 11.38 g (62.5%).

2.7.1.2 Conversion of Emeraldine Hydrochloride (~42% Protonation) to the fully protonated (~50%) hydrochloride

A portion of the product (~42% Protonation) was crushed into a powder and then equilibrated in 500 mL of 1M HCl for 15 hours. It was then filtered under suction and washed with 100 mL of 1M HCl. The filtrate was then allowed to dry overnight under suction. The yield of the product was 7.32 g (40.2%).

2.7.1.3 Synthesis of Emeraldine Base, EM

The 50% emeraldine hydrochloride (Section 2.7.1.2) was crushed into a powder and 500 mL of 0.1M NH_4OH solution was added to the mixture. The mixture was then stirred for 15 hours. The product was filtered, washed with 0.1 M NH_4OH solution, and dried under suction overnight. The yield of the EM was 5.39 g (29.6%).

2.7.1.4 Conversion of Emeraldine Base (EM) to Leucoemeraldine Base (LM)

Conversion of EM to LM was done under anaerobic and anhydrous conditions. EM base PANI was taken into a three-neck round bottom flask and dried under vacuum overnight to make the product air free and moisture free. A four-fold excess of anhydrous hydrazine (23 mL, 1M solution in THF) was added dropwise to the reaction flask over a period of 30 minutes. The reaction mixture was stirred for 20 hours under nitrogen flow, and the resultant product was filtered and washed with dry THF. During the addition of hydrazine to EM, the colour of the mass changed from black to blue. The excess THF was removed under vacuum at room temperature for a period of 20 hours. The yield of LM was very poor, 2.61 g (14.4%) because of significant loss of the product during handling.

2.8. Synthesis of Poly[(diPANI)phosphazene]

Three sites of polyaniline can be modified. These are the ortho and meta positions in the aromatic ring, and the amine group on the polymer chain. On the other hand, every repeating unit of PDCP has two chlorine atoms, which can be fully or partially replaced by electronegative ion(s), molecule(s) or group(s). Our aim was to synthesize a new polymer by replacing all chlorine atoms of the PDCP by PANI-LM salt. To achieve this, equimolar proportions of DMSO and NaH were allowed to react together to form methylsulfinyl carbanion(II) as mentioned in the literature[62].

$$CH_3\text{-}SO\text{-}CH_3 + NaH \longrightarrow CH_3\text{-}SO\text{-}CH_2^-Na^+ + H_2 \qquad (2.5)$$

This resulting methylsulfinyl carbanion was then reacted with PANI to form polyanilline-salt, which reacted with PDCP to form poly[(diPANI)]phosphazene . A proposed reaction scheme is illustrated in section 3.4.6.

Procedure

Sodium hydride (0.115 g, 0.005 mol) was taken into a round flask and treated with excess DMSO (40 mL, 0.56 mol) under nitrogen flow. The reaction flask was suspended in a 60°C water bath for six hours and manually shaken from time to time. At this stage, LM (0.40 g, 0.004 mol) was added in order to react with the methylsulfinyl carbanion(II) at 60°C. An immediate reaction was observed, as the colour of the reaction mixture was found to turn blue. The reaction was allowed to proceed for 5 hours at 60°C. The reaction vessel was

allowed to cool down to room temperature. A dark yellow solution was obtained, which was kept under nitrogen.

This dark yellow viscous solution was heated at 40°C in a water bath and $(PNCl_2)_n$ (1.29g, 0.11 mol) was added. Immediately, the dark-yellow solution changed into deep blue colour. The reaction was allowed to proceed for 64 hours with stirring and nitrogen purging. The excess DMSO was removed by freeze drying for 4 days resulting a blue-green material. Since the product was found to be insoluble in water at room temperature, it was washed with water till the $AgNO_3$ test showed no white precipitation. Thus, the by-product (NaCl) was removed from the mixture. After washing, the product was filtered out and dried under suction overnight. The yield of the final poly[(diPANI)]phosphazene was found to be 0.53 g (58.9%).

2.9. Preparation of lithiated molybdenum bronze

Lithiated molybdenum bronze was prepared by the reaction between molybdenum trioxide and n-BuLi as described by Equation 3. Molybdenum trioxide (6.14 g, 0.04 mol) was treated with an equal number of moles of n-BuLi (17 mL 2.5 M, 0.04 mol). The concentration of the n-BuLi was adjusted to 1M solution by adding dry pentane. The mixture was agitated for 50 minutes and then filtered under reduced pressure. The resultant dark blue product was dried for 1 hour under reduced pressure.

2.10. Preparation of POMOE/Li_xMoO_3 nanocomposite

An aqueous 2% w/v suspension of Li_xMoO_3 in deionized water (185 mg/10 mL, 0.0012 mol/10 mL) was sonicated for two hours and a saturated solution of POMOE (0.05 g, 0.0013 mol) in approximately 3 mL of deionized water was added to the suspension. The mass was stirred for three days at room temperature. It was then filtered, washed with deionized water and dried under reduced pressure.

2.11. Preparation of POEGO/Li_xMoO_3 nanocomposite

Li_xMoO_3 (0.206 g, 0.0014 mol) in 10 mL of deionized water was sonicated for two hours and a saturated solution of POEGO (0.071 g, 0.0015 mol) in 3 mL of deionized water was added to the above suspension. The resultant mixture was stirred at room temperature for 3 days and the composite material was filtered, washed thoroughly with water and dried under reduced pressure at room temperature.

2.12. Preparation of lithiated tin disulfide

Lthiated tin disulfide, Li_xSnS_2, was prepared by the redox reaction between SnS_2 and n-BuLi (Equation 2.3) in the dry box. An amount of 1.98 g (0.012 mol) of SnS_2 was taken into 250 mL Erlenmeyer flask and treated with three fold excess of n-BuLi (13.0 mL 2.5 M, 0.04 mol). The concentration of the n-BuLi was adjusted to a 1.0M through the addition of dry pentane. The mixture

was agitated for 50 minutes and then filtered under reduced pressure. The resultant orange-brown product was dried for 1 hour.

2.13. Preparation of POMOE/Li_xSnS_2 nanocomposite

A 2% w/v aqueous suspension of Li_xSnS_2 was sonicated for 30 minutes and a saturated solution of POMOE (0.09 g, 0.002 mol) was added to the suspension. The reaction mixture was sonicated for 4½ hours. The mixture was then stirred for three days at room temperature. The resulting reaction mixture was cast as a film on a glass substrate.

2.14. Preparation of POEGO/Li_xSnS_2 nanocomposite

The intercalation of POEGO in Li_xSnS_2 was performed following the same procedure as for the case of POMOE-Li_xSnS_2 reaction. A 2% w/v aqueous suspension of Li_xSnS_2 was sonicated for 30 minutes, and POEGO (0.09 g, 0.002 mol) dissolved in a minimum amount of deionized water (3 mL) was added to the suspension. The mixture was sonicated for 4½ hours followed by agitation for three days at room temperature. The resulting product was then cast as a thin film on a glass plate.

2.15. Synthesis of Graphite Oxide

Graphite oxide was synthesized according to Hummers method[63] as described in the literature.

2.15.1. Chemical reaction

The oxidation of graphite can be schematically described as follows:

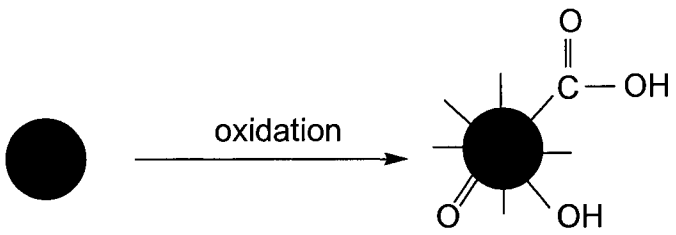

graphite graphite oxide

2.15.2. Procedure

Five grams of graphite powder was taken into a 4.0 L Erlenmeyer flask and 115 ml of precooled (0^0C) concentrated sulfuric acid was added to it. The mixture was stirred for a few minutes while maintaining the temperature below 20^0C. Fifteen grams of solid $KMnO_4$ was slowly added to the mixture and then stirred for half an hour, followed by the addition of 230 ml of deionized water, while keeping the temperature below 98^0C. Stirring was continued for another 15 minutes and the reaction was terminated by the addition of 50 ml of 30% H_2O_2, after dilution of the reaction mixture with 700 ml of water. The product was filtered, thoroughly washed with 1.4 M HCl to remove all sulfate ions. Finally the product was dried under vacuum and kept in the desiccator.

2.16. Preparation of POMOE/Graphite Oxide nanocomposite

The intercalation of POMOE was carried out in the following way. Graphite oxide (107 mg, $6.66*10^{-4}$ mol) and POMOE (26 mg, $6.08*10^{-4}$ mol) were placed

in 10 ml of deionized water and the mixture was sonicated for 30 minutes. The resulting suspension was stirred at room temperature for 24 hours. The pH of the suspension was then adjusted to 2 by the addition of 5 drops of concentrated HCl. Stirring was continued for another 24 hours. The reaction mixture was then heated at 60^0C for a period of 90 minutes and then cooled to room temperature. The excess polymer was thoroughly washed out with water. Finally, the composite was cast as a thin film on a glass substrate.

2.17. Determination of Molecular Weight of the Polymers by Viscometry

In a typical determination of average molecular weight (MW) by viscometry, poly(ethylene-glycol), PEG ranging from 2000 to 100000 were used as standard polymers. The retention time of these standard polymer solutions in water (0.5 g/100 mL) were determined from the following relationship,

$$\eta = (\eta_0 * t)/t_0 \qquad (2.6)$$

where, η_0 = viscosity of pure water[16]

η = viscosity of pure standard polymer

t_0 = retention time for pure water

t = retention time for standard polymer

The results were fitted in the Mark-Houwink equation,

$$\ln(\eta) = \alpha \ln(MW) + \ln(\kappa) \qquad (2.7)$$

A plot of ln(η) versus ln(MW) gave the calibration curve.

Table 2.2. Retention time for standard samples at 22^0C

Molecular Weight of Standard PEG	Average Retention Time (in second)
2000	76
3400	77
4600	78
8000	82
10000	85
100000	122
Retention time (in seconds) for pure water	
Pure water	70

The best-fit curve for the data (Table 2.2) was determined and the equation for that curve (linear equation) was derived.

$$\ln(\eta)\ (\pm\ 0.05) = (0.13 \pm 0.02)\ \ln(MW) - 0.99 \qquad (2.8)$$

$$[R^2 = 95]$$

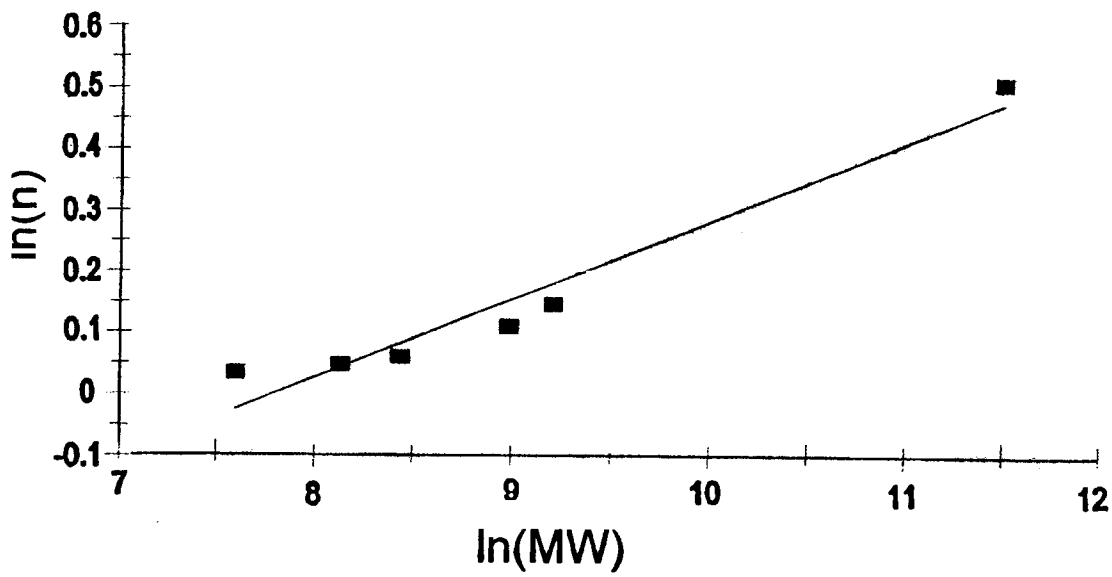

Figure 2.1. Mark-Houwink plot for standard polymers

This derived relationship could be considered as a general equation to determine the average molecular weight of a polymer dissolved in water. Aqueous solutions of POMOE, POEGO and MEEP (0.5g/100mL) were prepared and the average retention time of the polymer solutions were determined at 22^0C (Table 2.3). Inserting these values into Equation 2.8, molecular weights of POMOE, POEGO and MEEP were estimated as summarized in Table 2.3.

Table 2.3. Retention time for polymers and their molecular weight at 22^0C

Name of the Polymer	Ave. Retention Time (in second)	Ave. Molecular Weight
POMOE	100	22000 ± 5.4%
POEGO	80	5500 ± 5.4%
MEEP	78	3200 ± 5.4%

2.18. Methodology

FT-IR spectra were collected on a Perkin Elmer 1600 series spectrometer and NMR spectra were measured on a Bruker Avance 300 MHz spectrometer. Elemental analyses were done at the Canadian Microanalytical Service Ltd.

Thermogravimetric Analysis (TGA)

A thermogravimetric analyzer is a device that heats a sample and measures the weight loss or gain as a function of temperature and/or time. Generally, TGA is used to determine polymer degradation temperatures,

absorbed moisture level, residual solvent content, and composition of materials such as intercalated nanocomposites.

Powder X-ray Diffraction (XRD)

X-ray diffraction is one of the most important characterization techniques for the determination of the size and the shape of a unit cell. The X-ray radiation most commonly used is that emitted by copper (monochromatic light), of characteristic wavelength for K radiation (λ = 1.542 Å).

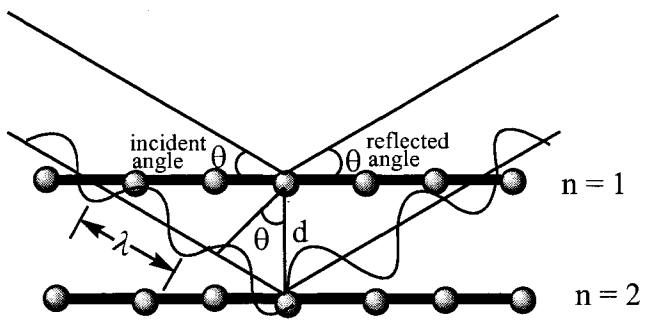

Figure 2.2. Diffraction of an X-ray beam satisfying the Bragg scattering condition

When the incident rays travel through a crystalline powdered sample, the scattering can be considered on the basis of interference of the waves that produce a cone of reflection with an angle of 2θ from the direction of the incident rays. Each reflection can be used to calculate the distance between two crystal planes i.e. the interlayer spacing (d-spacing) of a layered host system using the Bragg's equation,

$$n\lambda = 2d\sin\theta \qquad (2.9)$$

where,

n = an integer (1,2,3,.....)

λ = wavelength in Å (=1.542Å for copper)

θ = the diffraction angle in degrees

d = interatomic spacing in Å

The crystallite size of a material (D) can be estimated from its X-ray diffraction pattern by using the Scherrer equation,

$$D = (k\lambda * 57.3)/\beta_{½} \cos\theta \qquad (2.10)$$

where,

$\beta_{½}$ = peak width at half height in 2-theta degrees

θ = diffraction angle in degrees

k = constant that depends on the shape of the crystallites

If the shape of a nanocomposite intercalate is considered to be a perfect sphere, the value of k can be assigned to 0.9. The value 57.3 is the conversion factor for radians to degrees.

Chapter 3: Results and Discussion

3.1. Poly[oxymethyleneoxyethylene], POMOE

3.1.1. FT-IR Spectroscopy

The FTIR spectrum of POMOE as a pressed KBr pellet was examined. The result of the important peaks is shown in Table 3.1.

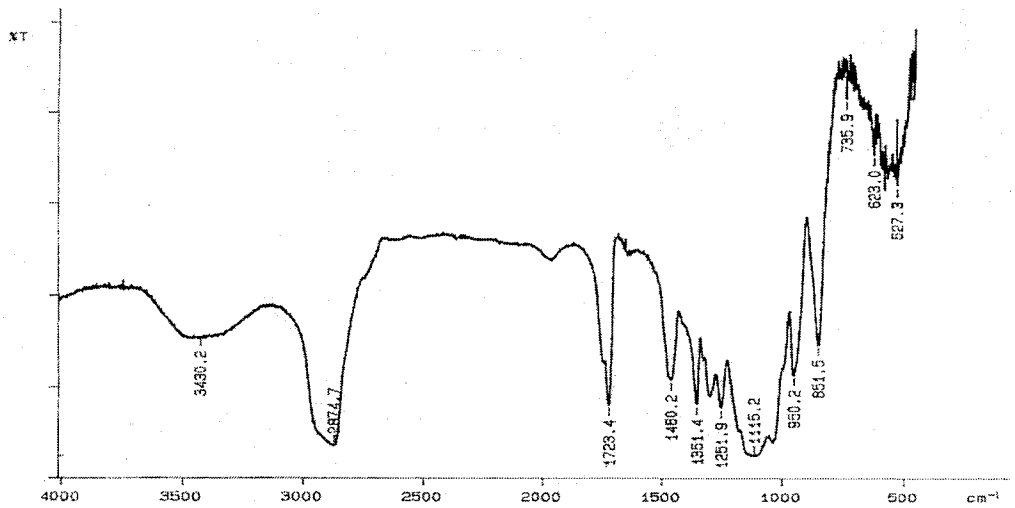

Figure 3.1. FT-IR of POMOE (64 scans)

3.1.2. NMR Spectroscopy

The ^{1}H NMR spectrum of POMOE (Figure 3.2.) showed peaks at 4.36 ppm (m) and 3.72 ppm (m) corresponding to $[-(OCH_2CH_2)_x-(OC\boldsymbol{H}_2)_{y-}]_n$ and $[-(O\boldsymbol{CH_2CH_2})_x-(OCH_2)_{y-}]_n$ and the integration indicates that there are 9 moles of $(OCH_2CH_2)_x$ (i.e. x = 9) for every $-(OCH_2)_y$ moles (i.e. y=1). From the structural point of view, it was expected that there would be triplets instead of multiplet peaks. Appearance of multiple peaks could be because of the fact that the

–CH_2– protons formed clouds in the polymer matrix and each proton signal was affected by many nearby protons rather than single –CH_2– group.

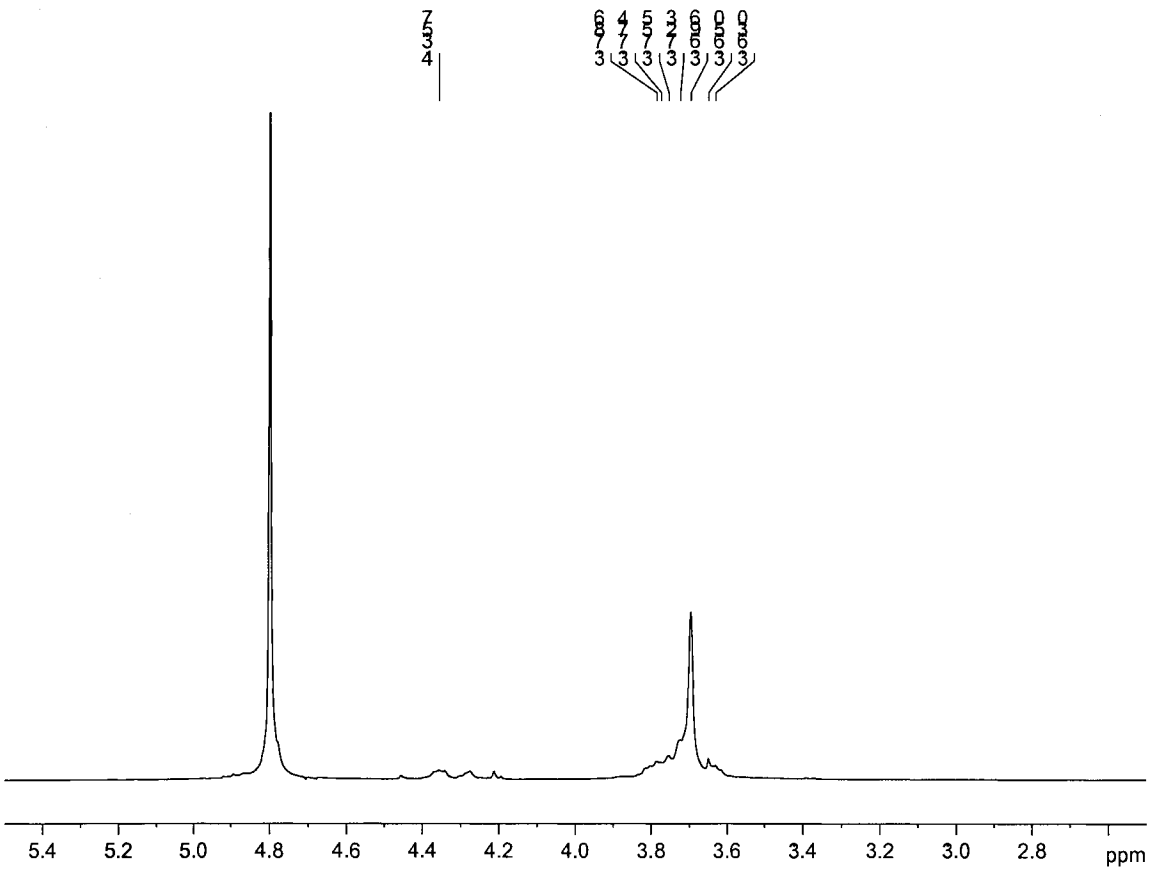

Figure 3.2. ^{1}H NMR of POMOE

3.1.3. Molecular Weight and Yield

The molecular weight of POMOE was determined to be $2.2*10^4 \pm 5.4\%$ by viscometry (section 2.17), and did not agree with the reported value of 10^5 as determined by GPC[48]. Lower molecular weight of the polymer might be possible if the reaction terminates earlier than the case described in the literature. As

mentioned earlier (Section 2.3.1), the yield of POMOE was not determined since only a portion of the crude POMOE was purified.

3.2. Poly[oligo(ethylene glycol) oxalate], POEGO

3.2.1. FT-IR Spectroscopy

The sample was run as a pressed KBr pellet. The major peaks are presented in Table 3.1.

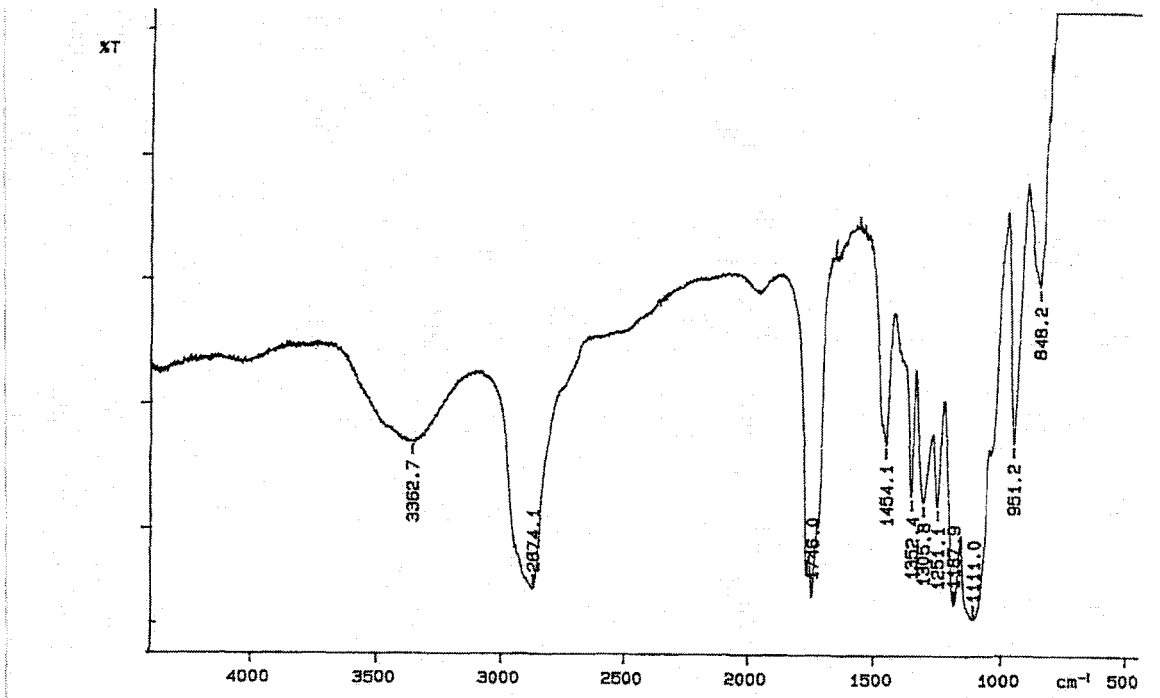

Figure 3.3. FT-IR of POEGO (64 scans)

Table 3.1. Significant FT-IR peaks for POMOE and POEGO

Major Bond/group	POMOE cm^{-1}	POEGO cm^{-1}
O-H	3430	3371
C-H	2874	2874
C-O/C=O	1723	1746
C-C	1460	1454
C-O-C	1115	1111

3.2.2. NMR Spectroscopy

^1H NMR in D_2O

The resonances in ^1H NMR spectrum at 4.51, 3.89 and 3.72 ppm are assigned to the protons of methylene ($-CH_2-$) group in –C(O)- C(O)-O-C***H***$_2$, – C(O)- C(O)-O-CH_2-C***H***$_2$ and –C(O)- C(O)-O-CH_2-CH_2-(O***CH$_2$CH$_2$***)$_{n-2}$-O- groups, respectively. These are close to their corresponding literature values[18]. The peak at 4.82 ppm is from the deuterated solvent (D_2O).

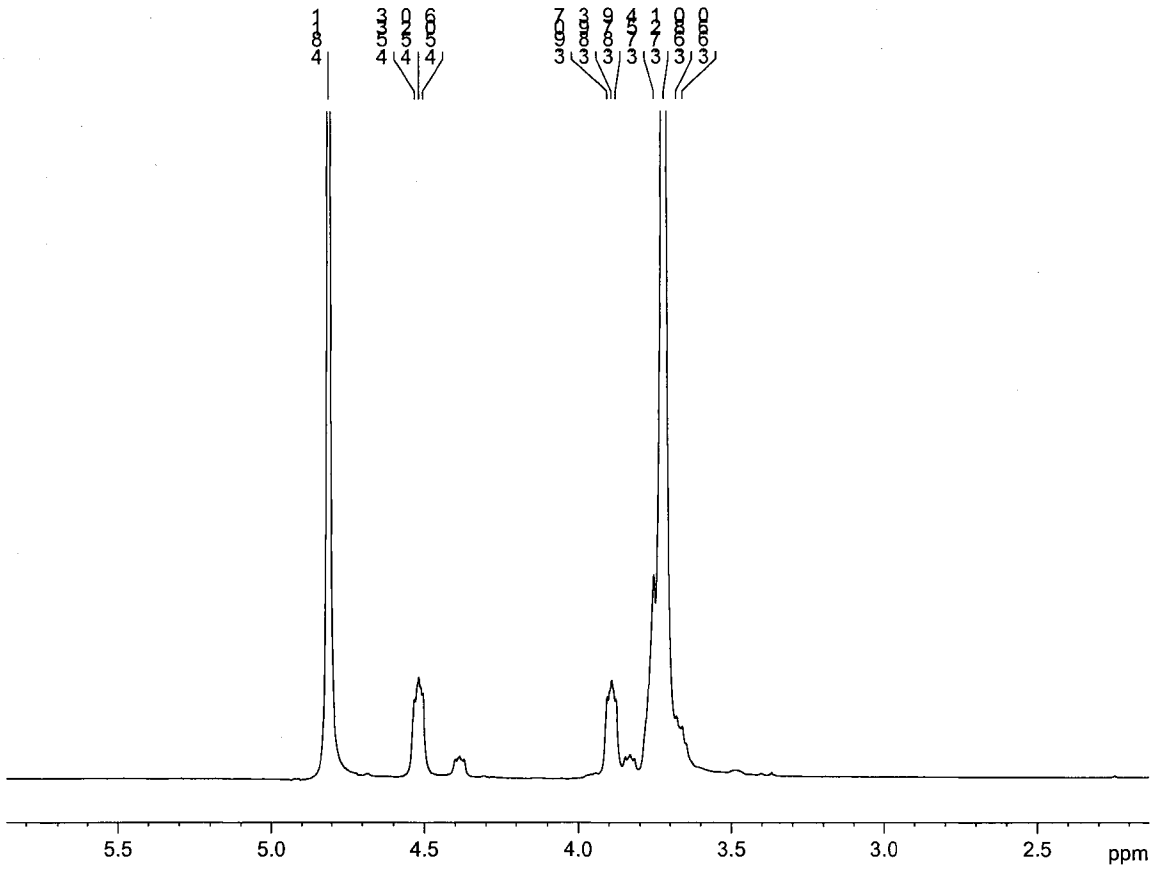

Figure 3.4. ^{1}H NMR of POEGO

^{13}C NMR in D_2O

In the ^{13}C NMR spectrum, the peak at 69.92 ppm is attributed to the carbon – C(O)- C(O)-O-CH_2-CH_2-(O***CH_2CH_2***)$_{n-2}$-O- groups. This value is very close to the literature value of 70.33 ppm[49].

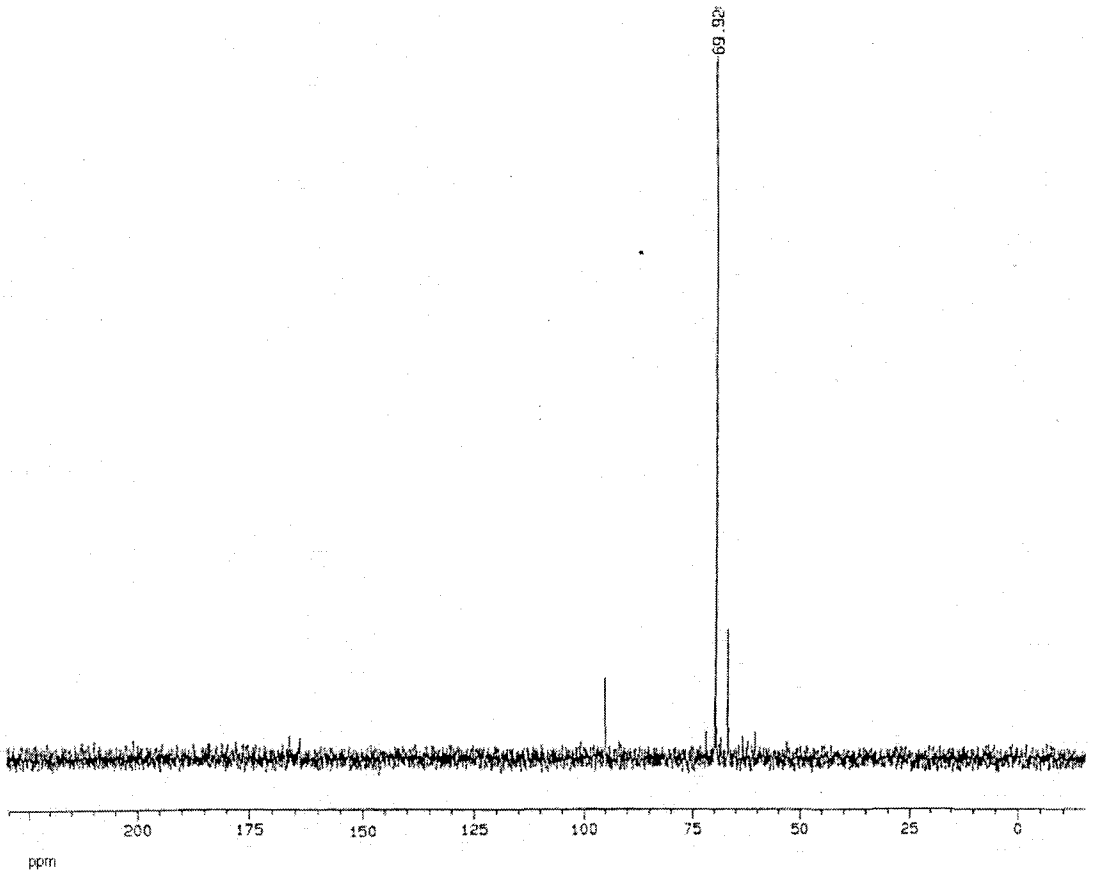

Figure 3.5. ^{13}C NMR of POMOE

3.2.3. Molecular Weight and Yield

The average molecular weight of POEGO was estimated to be 5500 ± 5.4% (section 2.17) that falls in the range of 3500 to 6800 as described in the literature[48]. The yield of the product was found to be 84.9%, which is in good agreement with the reported value of 94.1%.

3.3. Poly[bis(2-(2′-methoxyethoxy)ethoxy)phosphazene] (MEEP)

3.3.1 Modified Route for the Synthesis of MEEP

The synthesis of MEEP according to the modified procedure was successful and reproducible. It was observed that the reaction between MEE and NaH was complete in 3 hours at room temperature, while it took at least two weeks if Na-pellet was used instead of NaH.

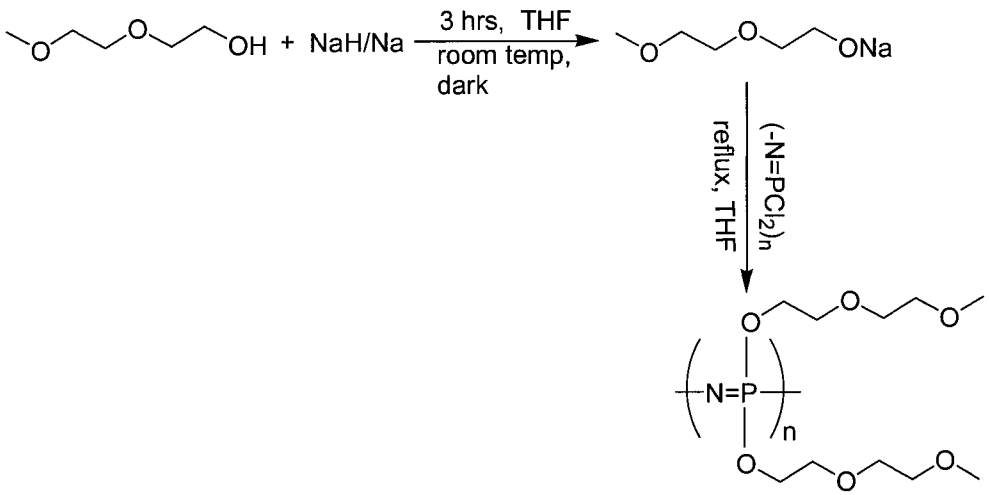

Scheme 3.1. Synthesis of MEEP using PDCP (scheme 2.3)

The product obtained in Scheme 3 was characterized by ^{1}H and ^{31}P NMR spectroscopy and the substitution of chlorine atoms were qualitatively determined by $AgNO_3$ test during purification of the product.

3.3.2. NMR Spectroscopy

The PDCP ^{31}P NMR spectrum showed only one peak at –17 ppm (Figure 3.6) as expected[58], which disappeared after substitution reaction between MEENa and PDCP (Figures 3.7, 3.8). The resultant product was air

stable and totally soluble in water at room temperature, a characteristic of MEEP as described in the literature[64]. Analysis of the crude product by ^{31}P NMR spectroscopy (Figure 7) showed a peak at -5.46 ppm, which is an indication of the presence of $N=P(OCH_2CH_2)_2OCH_3$[65]. The other significant peak at 18.6 ppm can be ascribed to the formation of trimer due to macrocondensation of PDCP over time at temperatures above 0^0C as reported in the literature[65]. However, ^{31}P NMR on the product after dialysis and freeze drying gave a clear singlet at -5.46 ppm due to the presence of $N=\mathbf{P}(OCH_2CH_2)_2OCH_3$ side groups (Figures 3.7, 3.8). Disappearance of other peaks is reasonable because of the lower molecular weight impurities that were washed out through the pores of the dialysis bags.

Further evidence for the structure of MEEP was determined by the ^1H NMR spectroscopy. The peaks between 3.37 and 4.2 ppm represent the protons of the MEE group (Figures 3.9, 3.10). Interestingly, the position and the pattern of the peaks were almost identical to the literature [64,66], for the -$OCH_2CH_2OCH_2CH_2$-CH_3 substitutents. ^1H NMR in D_2O: δ 3.37 (s, $OCH_2CH_2OCH_2CH_2.\mathbf{CH_3}$), 3.35-3.38 (m, $OCH_2\mathbf{CH_2}O\mathbf{CH_2}\mathbf{CH_2}CH_3$), 4.15 (br, P-O-$\mathbf{H_2}CH_2OCH_2CH_2CH_3$).

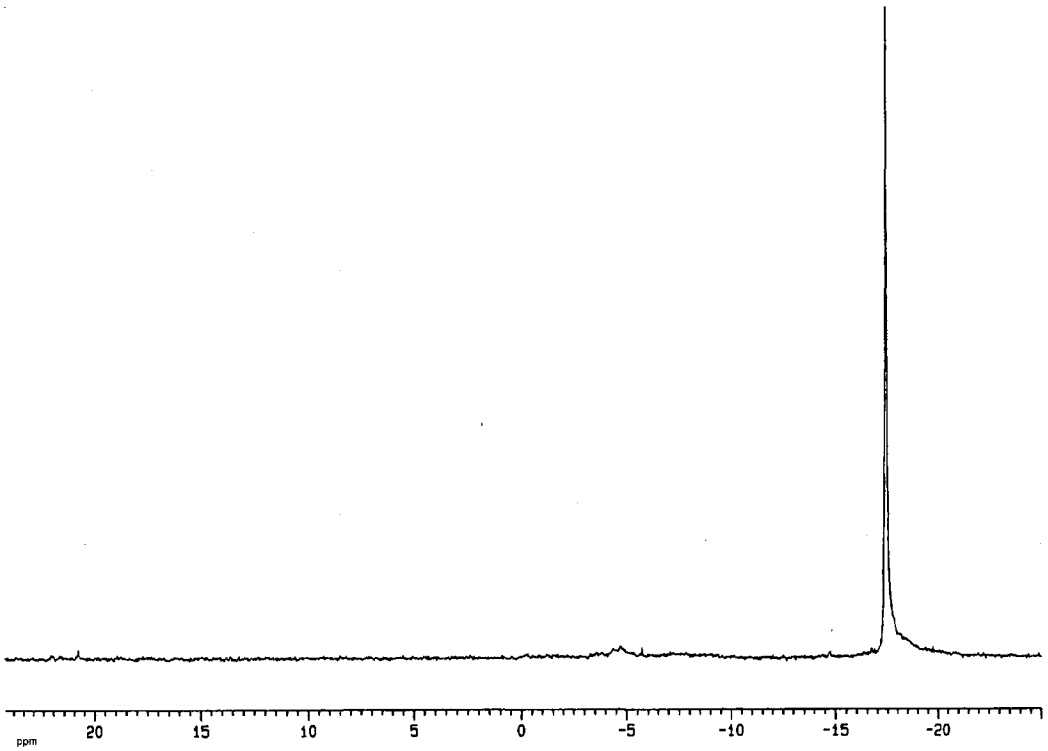

Figure 3.6. ^{31}P NMR of PDCP

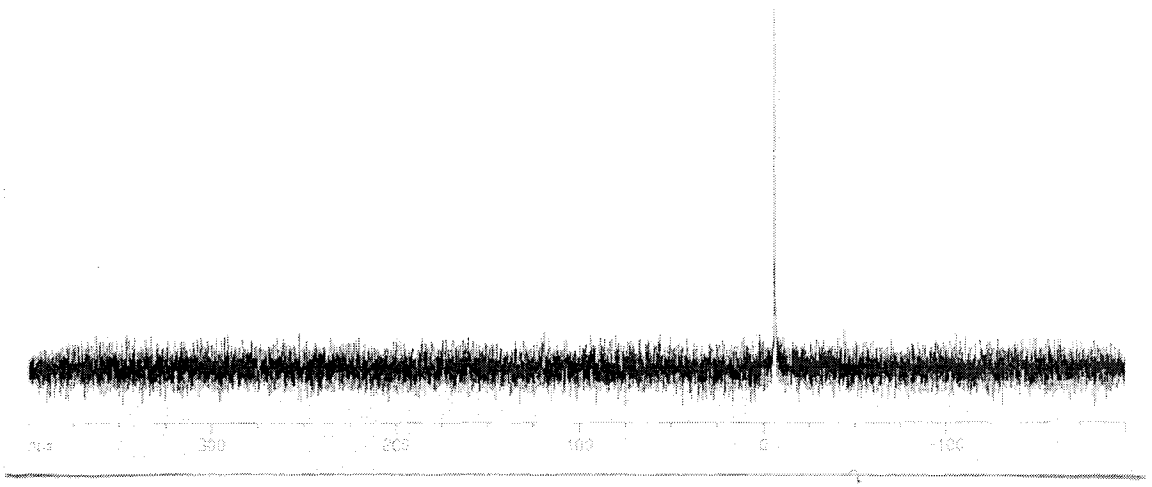

Figure 3.7. ^{31}P NMR of MEEP (final product)

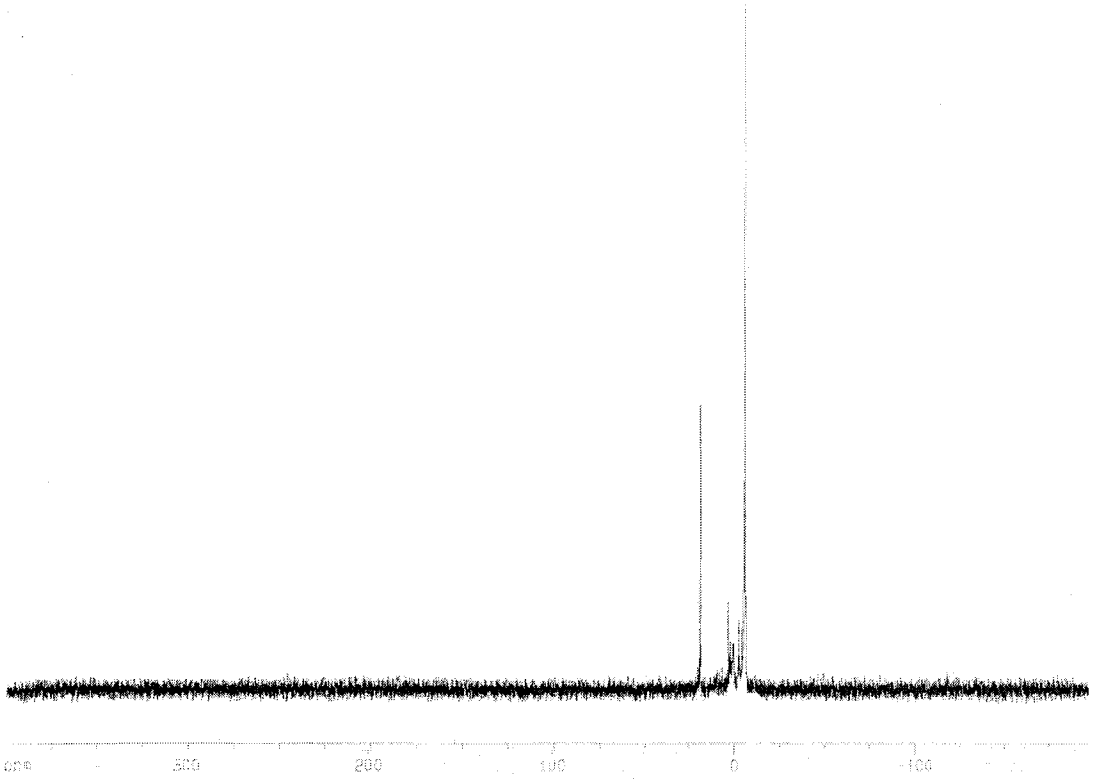

Figure 3.8. ^{31}P NMR of crude MEEP (before dialysis)

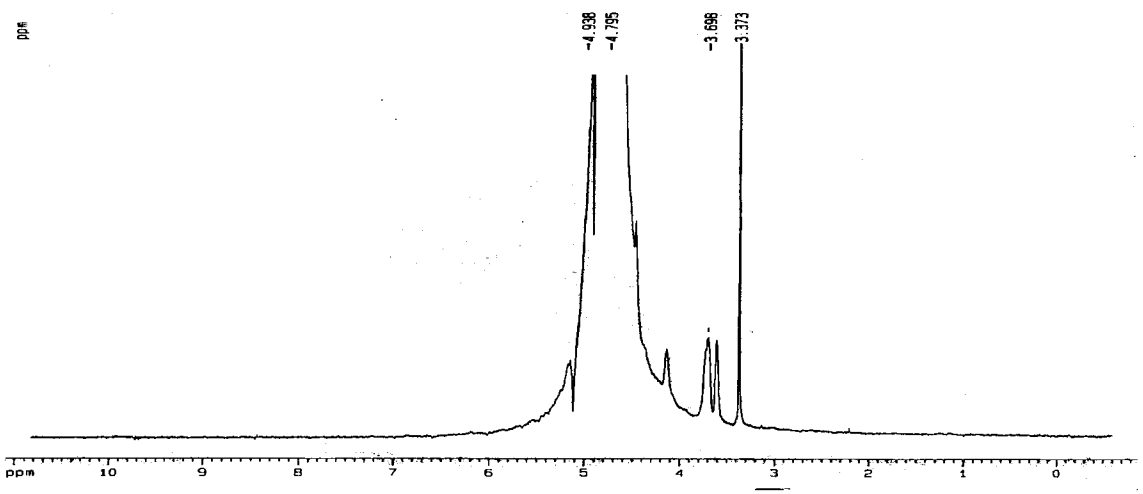

Figure 3.9. ^{1}H NMR of MEEP (final dialysis)

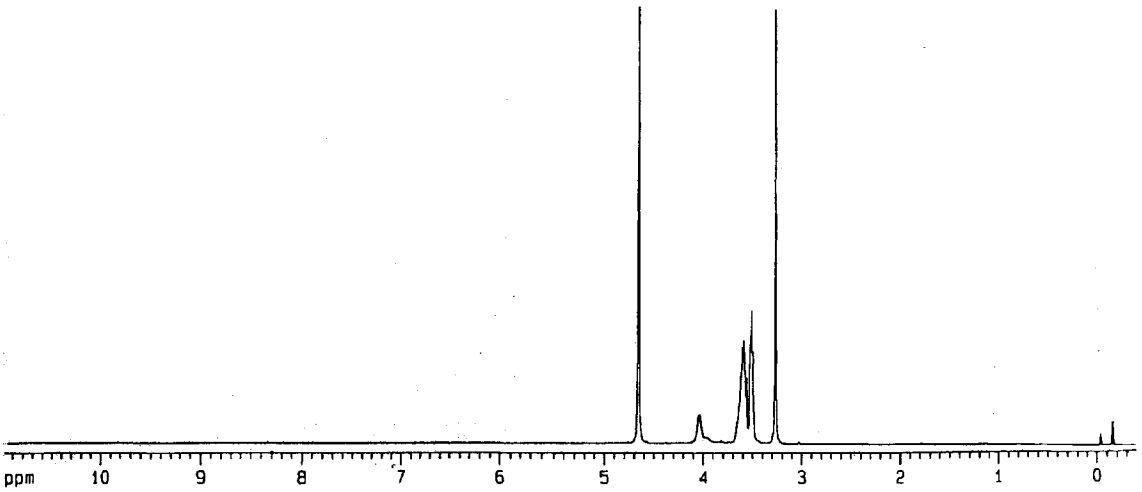

Figure 3.10. ^{1}H NMR of crude MEEP (before dialysis)

3.3.3. Molecular weight and Yield

The molecular weight (MW) of MEEP was determined to be 3200 ± 5.4% at 22^{0}C (section 2.17). This value is low maybe because of the fact that MW of PDCP was low. Simple modification of the procedure *i.e.* use of PCl_3 and SO_2Cl_2 solutions in CH_2Cl_2 instead of $PCl_{3(liquid)}$ and $SO_2Cl_{2(liquid)}$ did not show any presence of $Cl_3P{=}NSiMe_3$ (s, -53 ppm), which can control the molecular weight of the polymer species as reported by the Manners group[59]. In addition, the retention time for MEEP was measured on a different day, where the room temperature and other settings of the apparatus may be different, but the standard data values shown in Table 2.2 were used for the calculation, which might produce a significant error in the result. The yield of MEEP was determined to be 71.3%, which was very close to the value reported in the literature[59]. The yields of the precursor, PDCP were 65.7%

and 60.6%, synthesized by ring opening polymerization method and the low temperature method, respectively, which were also found to be closer to the reported values.

3.4. Poly[(diPANI)phosphazene]

The characterization of the product was done by solubility test, physical test, FT-IR and NMR spectroscopies.

3.4.1. Solubility Test

The solubility of the product was examined using 11 solvents. In each case, the solubility was tested in three different ways:

(i) A small portion of the product was taken into a test tube and solvent was added and shaken manually.

(ii) If not soluble, the test tube (i) was sonicated at room temperature for 30 minutes

(iii) If not soluble, the test tube (ii) was sonicated at 50^0C for 45 minutes.

The results from these experiments are shown in Table 3.2.

Table 3.2. Solubility of Poly[(diPANI)phosphazene]

Solvent	**Manually shaken (r.t.)**	**Sonication (30 mins at r.t.)**	**Sonication (45 mins at 50^{0}C)**
Acetonitrile	NS	NS	NS
Benzene	NS	NS	NS
Chloroform	NS	NS	NS
DMSO	NS	NS	NS
Ethanol	NS	NS	NS
Ether	NS	NS	NS
Hexane	NS	NS	NS
Methanol	NS	NS	PS**
Pyridine	NS	NS	NS
THF	NS	NS	NS
Water	NS	NS	S*

Notations:
NS = not soluble, S* = soluble, PS** = partially soluble, r.t. = room temperature, mins = minutes

It was found that the product was soluble in water at around 50°C with the aid of sonication. But if the solution was cooled down to room temperature and kept overnight without any disturbance, the product would precipitate out. MeOH was in second position in terms of solubility under the same conditions as water.

The solubility characteristic of the Poly[(diPANI)phosphazene] is not clearly understood. The PDCP backbone can be considered to be hydrophilic, primarily due to the presence of the nitrogen lone pair electrons and their ability to form hydrogen bonds to water molecules. However, the net hydrophilic or hydrophobic property can be justified by the side groups and by the degree to which they shield the skeleton. MEEP is soluble in water because the MEE side groups themselves are hydrophilic. It was assumed that hydrophobic PANI

groups in Poly[(diPANI)phosphazene] could hide the PDCP backbone. Surprisingly, the product was found to be soluble in some polar solvents such as water and methanol. However, as the size of the polar molecule increases, the solubility decreases. Thus, the compound was found to be less soluble in methanol than water and insoluble in ethanol under the same conditions. The product may behave like PANI as the product is insoluble in most of the common organic solvents.

3.4.2. FT-IR Spectroscopy

The FT-IR spectra of PANI (EM) and Poly[(diPANI)phosphazene] are shown in Figure 3.11 and Figure 3.12, respectively. The characteristic vibrations of PANI are clearly observed. The observed bands at 1556 cm^{-1} (C-C ring stretching), 1292 cm^{-1} (C-H bending), 1108 cm^{-1} (in plane C-H bending) and 802 cm^{-1} (out of plane C-H bending) are closely related to the corresponding literature values of 1292 cm^{-1}, 1109 cm^{-1} and 797 cm^{-1}. The bands at 3430 cm^{-1} and 2923 cm^{-1} originate from the C-H and NH_2 groups. The band for NH_2 group in Poly[(diPANI)phosphazene (Figures 3.12) disappeared completely because of the formation of new N-P-N bonds, which was expected. In addition, a significant shift of all the bands in the range of 1599 cm^{-1} to 976 cm^{-1} from 1556 cm^{-1} to 802 cm^{-1} was observed because of new arrangement of PANI attached to PDCP backbone. Bands at 1207 cm^{-1}, 1154 cm^{-1} might be due to the P-N vibration.

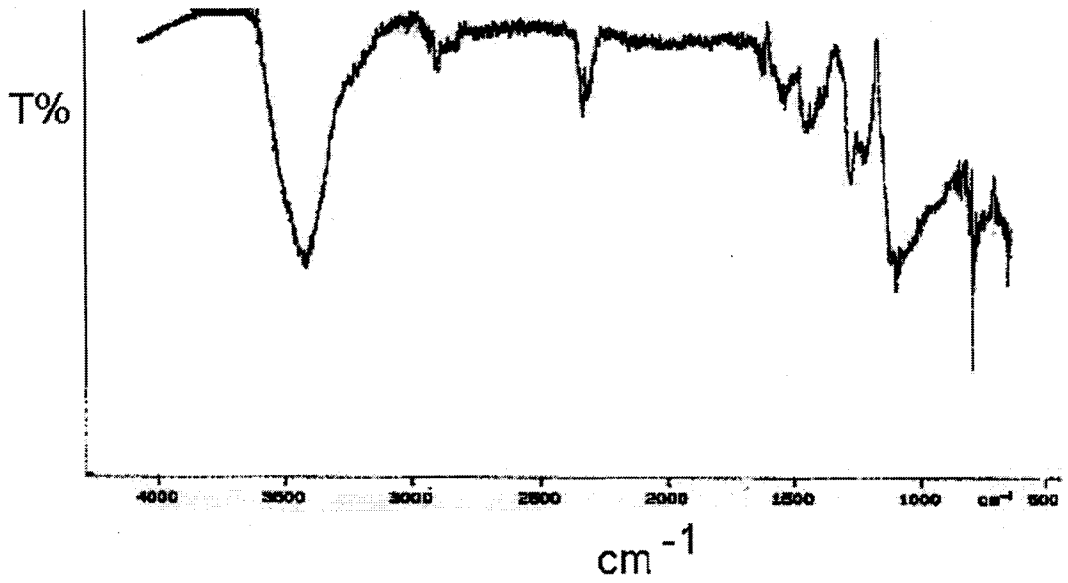

Figure 3.11. FT-IR of PANI (EB) (64 scans)

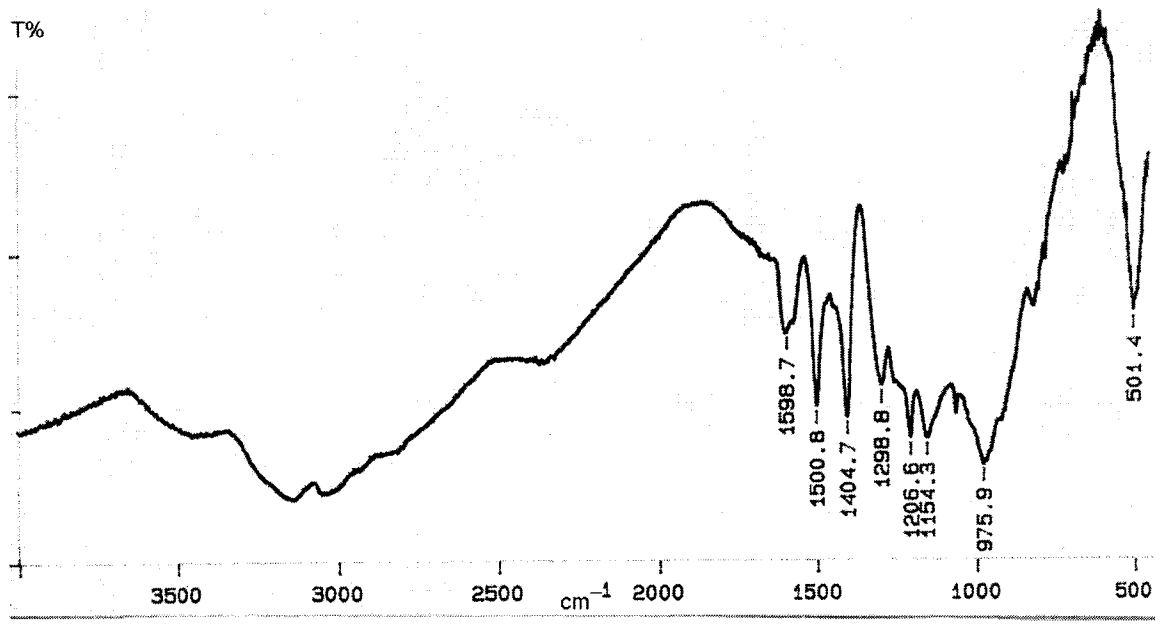

Figure 3.12. FT-IR of Poly[(diPANI)phosphazene] (64 scans)

3.4.3. Determination of Crystaiiinity by XRD

The X-ray powder diffraction pattern was run on a D4Endeavor XRD using Cu tube of radiation (wavelength =1.542 Å) operated at 40 kV and 50 mA. The product was found to be amorphous because a very broad signal was observed. This indicated the absence of regular arrangement of the repeat units. The conditions for microcrystallinity in polyphosphazene can only be met when homogeneous side groups are present and when those side groups are small or fairly rigid. When heterogeneous side groups are present, the macromolecules usually lack the necessary symmetry and regularity. The PANI side groups are large and possibly flexible enough to meet the amorphous characteristic of Poly[(diPANI)phosphazene.

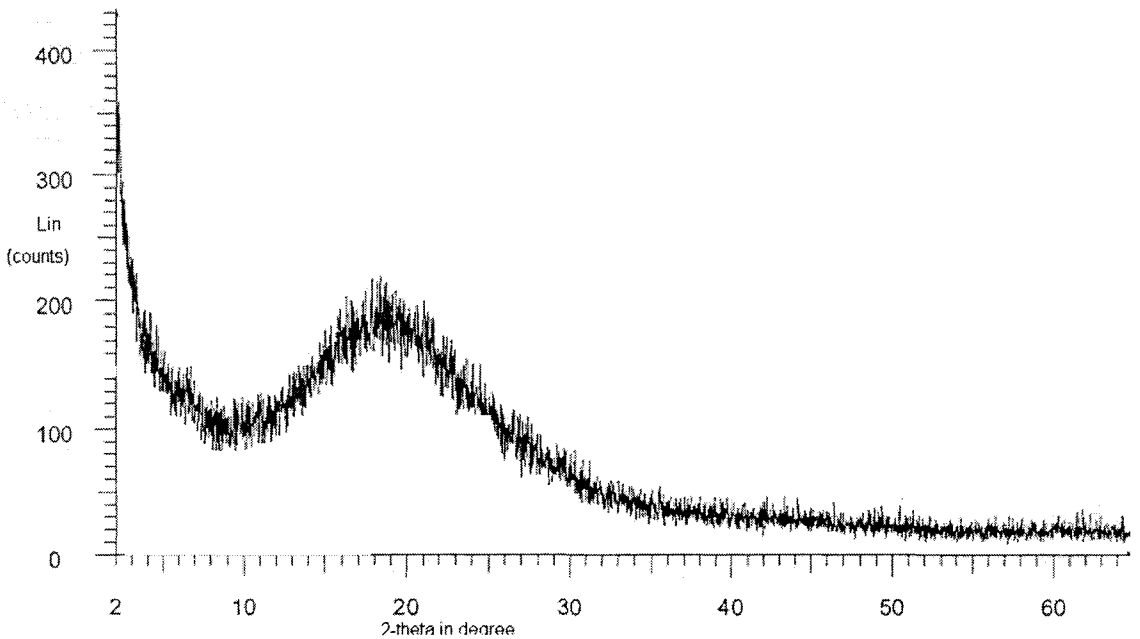

Figure 3.13. XRD of poly[(diPANI)phosphazene]

3.4.4. Proposed Reaction

As mentioned earlier, attempts were taken to replace chlorine atoms from the PDCP backbone by the following reactions:

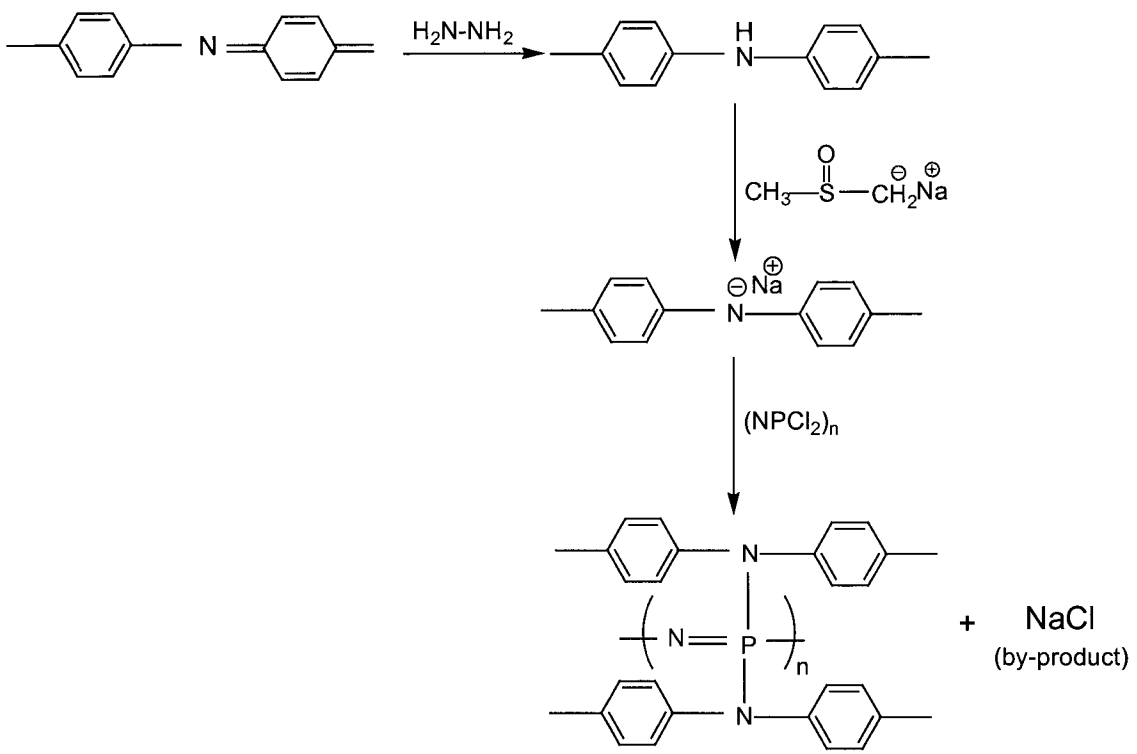

Scheme 3.2. Proposed reaction between active anion of polyaniline salt and dichlorophosphazene

3.4.5. Identification of the by-product

Sodium chloride was found to be the by-product of the synthesis as determined by a qualitative silver nitrate test. Although this is a trivial method, it supports the proposed substitution of chlorine atoms by the reaction as shown in the Scheme 3.2.

3.4.6. NMR Spectroscopy

The ^{31}P NMR spectrum of the product in D_2O at 50^0C showed only one singlet peak as expected at 1.21 ppm indicating the formation of a new product. There was no peak found at –17 ppm, which means all PDCP went into reaction. The upfield shift of the peak (from –17 ppm to 1.21 ppm) was also expected because chlorine in PDCP is more electronegative than nitrogen in P-N bond of the new polymer.

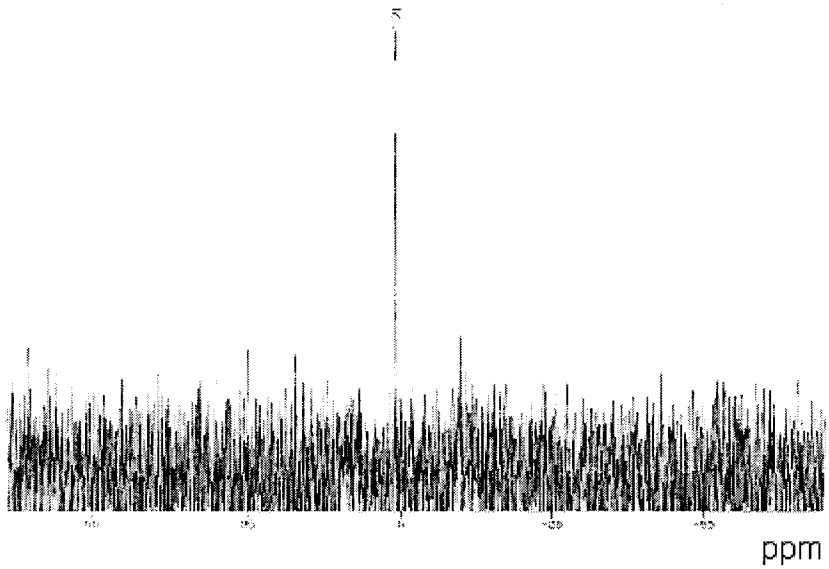

Figure 3.14. ^{31}P NMR of substituted PDCP with PANI

3.5. POMOE/Li_xMoO_3 Intercalate

3.5.1. Reaction

Lithium ions were introduced into the MoO_3 host by a redox reaction between MoO_3 and n-BuLi according to the following reaction,

$$MoO_3 + xC_4H_9^-Li^+ \longrightarrow \overset{\oplus}{Li}_x\overset{x\ominus}{MoO_3} + {}^1/_2\, x\, C_8H_{18} \qquad (3.1)$$

where the MoO_3 layer was reduced to MoO_3^{x-} (Figure 3.15b)

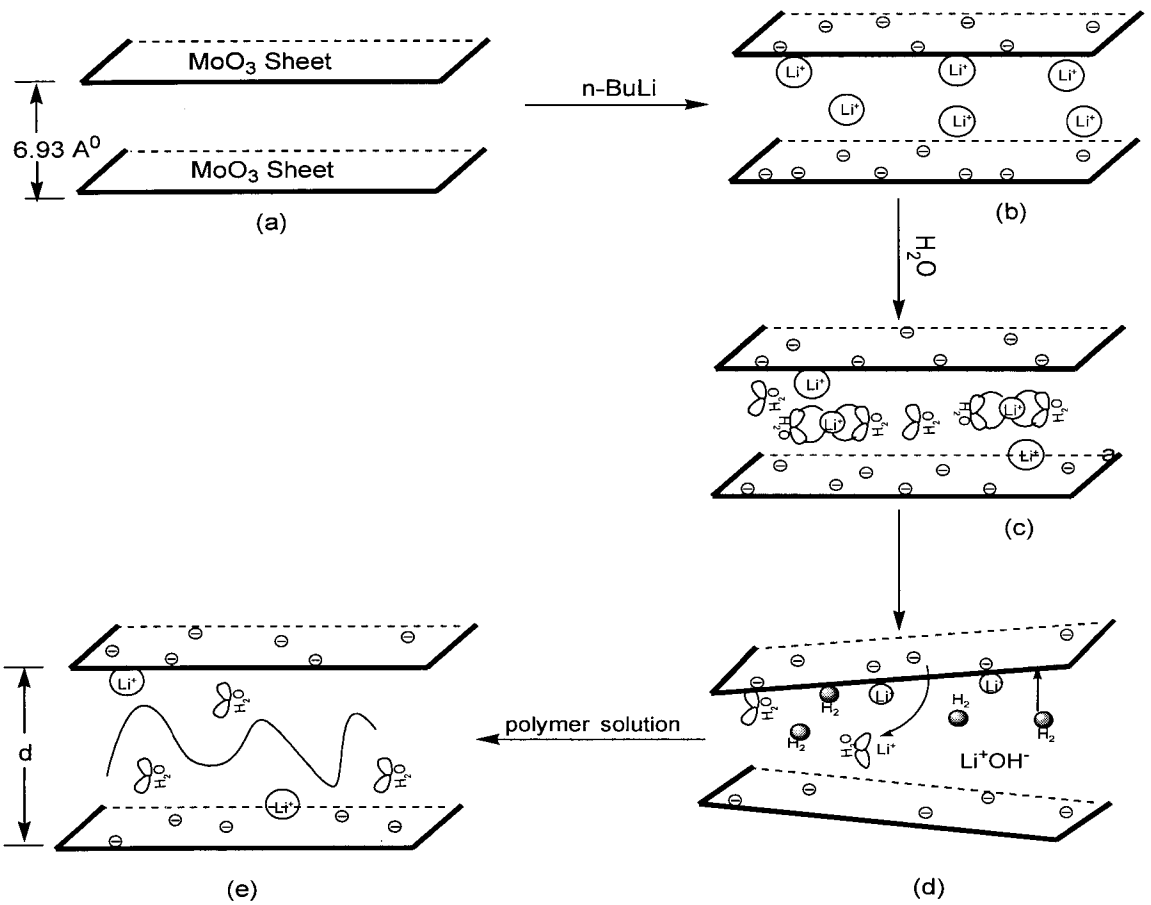

Figure 3.15. Proposed reaction mechanism for the intercalation of POMOE and POEGO into MoO_3 (a) Pristine MoO_3 with d-spacing 6.93Å (b) insertion Li^+ into MoO_3 (c) hydrated Li_xMoO_3 phase (d) swelling of the MoO_3 plates (e) restacking of the MoO_3 layers.

It is assumed that in aqueous media, some electrons from the reduced MoO_3^{x-} were transferred to the co-intercalated water to form LiOH and H_2. Exfoliation/restacking method was employed to include POMOE and POEGO in MoO_3. This is somewhat similar to the encapsulation of guest molecules into the MoS_2 layered system[67]. Reaction between Li_xMoO_3 phase and water results in swelling of the MoO_3 layers (Equation 3.2). In addition, sonication helps to complete the swelling process.

$$Li_xMoO_3 + yH_2O \longrightarrow \underset{\text{swelled layers}}{\left(Li_{(x-y)}MoO_3\right)} + yLiOH + \uparrow {}^{y}/_{2}H_2 \qquad (3.2)$$

The polymers when added to the system entered in between the expanded layers. The layers restacked with the polymer trapped between the host resulting in the formation of intercalated nanocomposites. For simplicity, co-intercalated water is not shown in the reactions.

$$\underset{\text{swelled layers}}{\left(Li_xMoO_3\right)} + y\,POMOE \longrightarrow Li_x\left(POMOE\right)_yMoO_3 \qquad (3.3)$$

$$\underset{\text{swelled layers}}{\left(Li_xMoO_3\right)} + z\,POEGO \longrightarrow Li_x\left(POEGO\right)_zMoO_3 \qquad (3.4)$$

With knowledge of the interaction between lithium ions and PEO as described in the literature[68], it can be assumed that the partially charged negative pole of the polymer feels a force of attraction for the lithium ions and probably forms POMOE-Li^+ and POEGO-Li^+ complexes.

3.5.2. FT-IR Spectroscopy

FT-IR spectra of POMOE/MoO_3 (Figure 3.16) and POEGO/MoO_3 (Figure 3.17) were collected as pressed KBr pellets. The results from the significant bands are summarized in Table 3.3.

Table 3.3. Significant FT-IR peaks for POMOE/MoO_3 and POEGO/MoO_3

Major Bond/group	POMOE/MoO_3 cm^{-1}	POEGO/MoO_3 cm^{-1}
O-H	3425	3424
C-H	2900	2919
C-O/C=O	1625	1631
C-C	1454	1430
C-O-C	1089	1093

From the above FT-IR results (Table 3.1 and 3.3), we can access the following information. First, upon intercalation, the FT-IR of the nanocomposites showed characteristic vibrations of POMOE or POEGO. This was expected because of the fact that the functional groups of the encapsulated polymer molecules were not modified. Second, it was observed that the peaks for virgin POMOE and POEGO occurred at higher wavenumbers compared to POMOE/MoO_3 and POEGO/MoO_3 systems. This could be due to an increase in reduced mass (μ) upon intercalation, which allowed the intercalated systems to vibrate at lower frequencies than the virgin polymers.

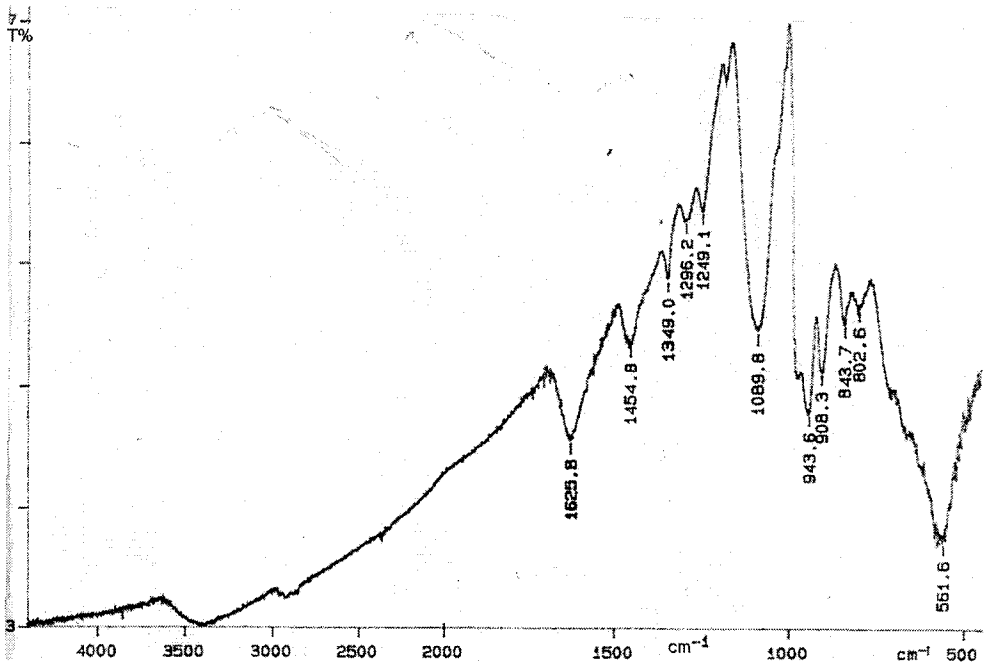

Figure 3.16. FT-IR of $LiMoO_3$/POMOE intercalate (64 scans)

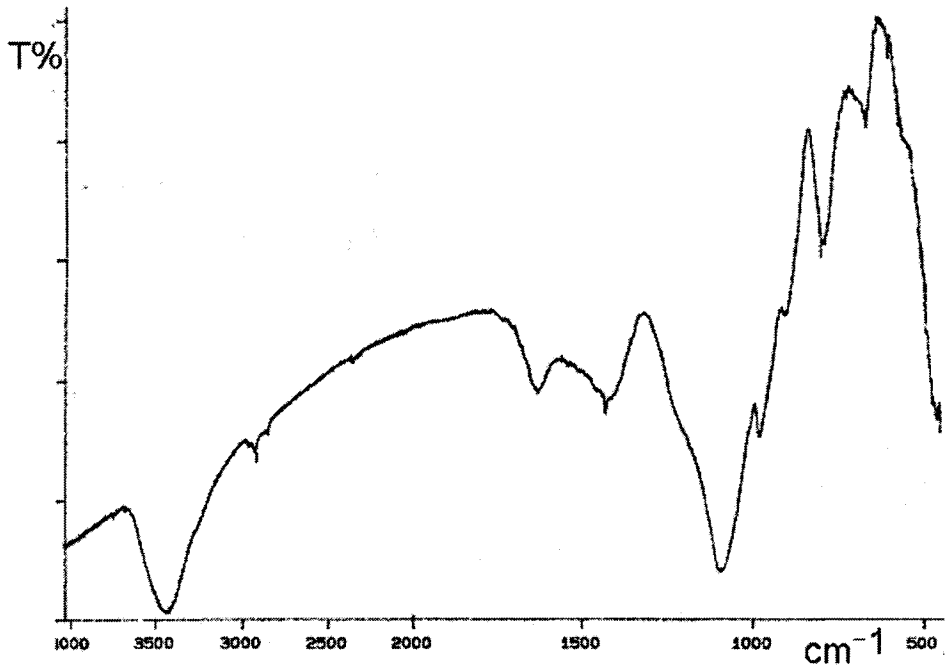

Figure 3.17. FT-IR of $LiMoO_3$/POEGO intercalate (64 scans)

3.5.3. Powder X-ray Diffraction

Powder X-ray diffraction (XRD) pattern of POMOE/MoO_3 showed 00*l* reflections, consistent with a layered structure. The first peak was observed at a 2θ value of 6.0 Å. Using the Bragg law (Equation 2.9), the calculated d-spacing value for the nanocomposite was 14.73 Å. The d-spacing of pristine MoO_3 is 6.93 Å. Therefore, the interlayer expansion of the host is 7.80 Å.

Similarly, the XRD of the POEGO/MoO_3 system showed 00*l* reflections, which confirmed the layered characteristic of the nanocomposite. The first peak was observed at a 2θ value of 6.25. The estimated d-spacing value of the nanocomposite was 14.14 Å, which corresponds to an interlayer expansion of 7.21 Å. On the basis of the XRD results, it can be assumed that there is a bilayer of the polymer chains trapped between the MoO_3 layers as shown in Figure 3.18.

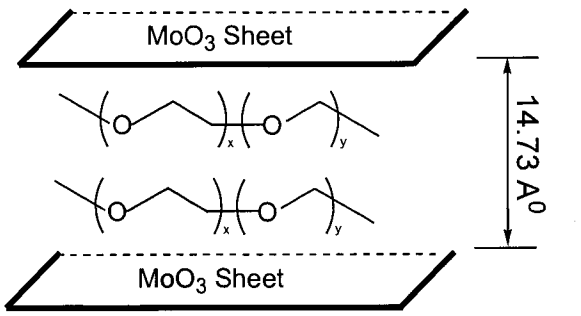

(a)

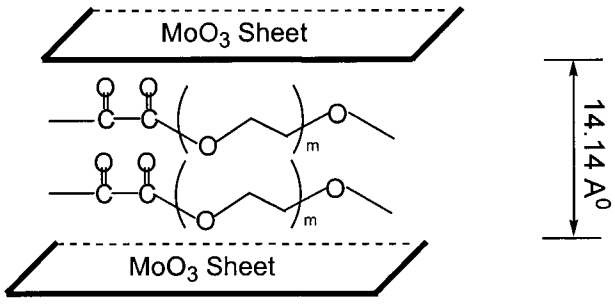

(b)

Figure 3.18. Schematic illustration of the proposed structure of (a) (POMOE)/MoO_3 intercalate (b) (POEGO)/MoO_3 intercalate

This insertion into MoO_3 can be compared with insertion of the above polymers into neutral MoS_2 system, where the d-spacing values for POMOE/MoS_2[32] and POEGO/MoS_2[9] were reported as 15.78 Å and 14.73 Å, respectively with corresponding interlayer expansion of 9.63 Å and 8.58 Å to accommodate bilayers of both polymers. The expansion of the MoO_3 layers also depends of the molecular weight of the polymers as reported by the Kanatzidis group[31]. This group intercalated PEG with different molecular weight and found that d-spacing for PEG/ MoO_3 (PEG, MW 2000) was 13.8 Å and 16.8 Å for PEG/ MoO_3 (PEG, MW 100000). POMOE and POEGO are similar to PEG in terms of

polarity. We estimated that the molecular weight of POMOE (MW 22000 ± 5.4%) and POEGO (MW 5500 ± 5.4%) are within the range of 2000 to 100000. Therefore, the d-spacing for POMOE/MoO_3 (14.73 Å) and POEGO/MoO_3 (14.14 Å) systems were found to be in good agreement with the PEG/MoO_3 system, reported by Kanatzidis [31]. Since MoO_3 was partially reduced, the polar molecules (POMOE/POEGO) feel strong electrostatic force, which was not the case for POMOE/MoS_2 and POEGO/MoS_2.

The crystallite size of the intercalates was estimated from their X-ray diffraction patterns by using the Scherrer equation (Equation 2.10). The average crystallite sizes of POMOE/MoO_3 and POEGO/MoO_3 were estimated to be 96 Å and 106 Å, respectively. The crystallite size of MoO_3 was estimated to be 640 Å. The reduction of crystallite size upon intercalation by 7.5 fold for POMOE/MoO_3 and 6 fold for POEGO/MoO_3 can be justified as improper restacking of the MoO_3 layers compared to its virgin structure.

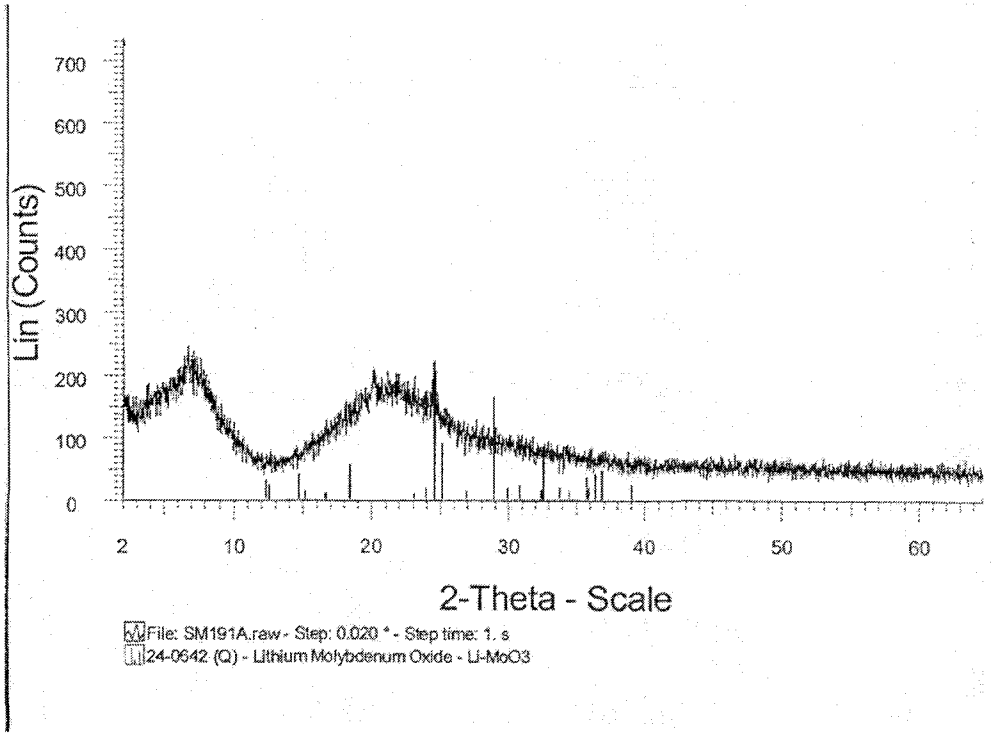

Figure 3.19. XRD of restacked MoO_3/H_2O intercalate

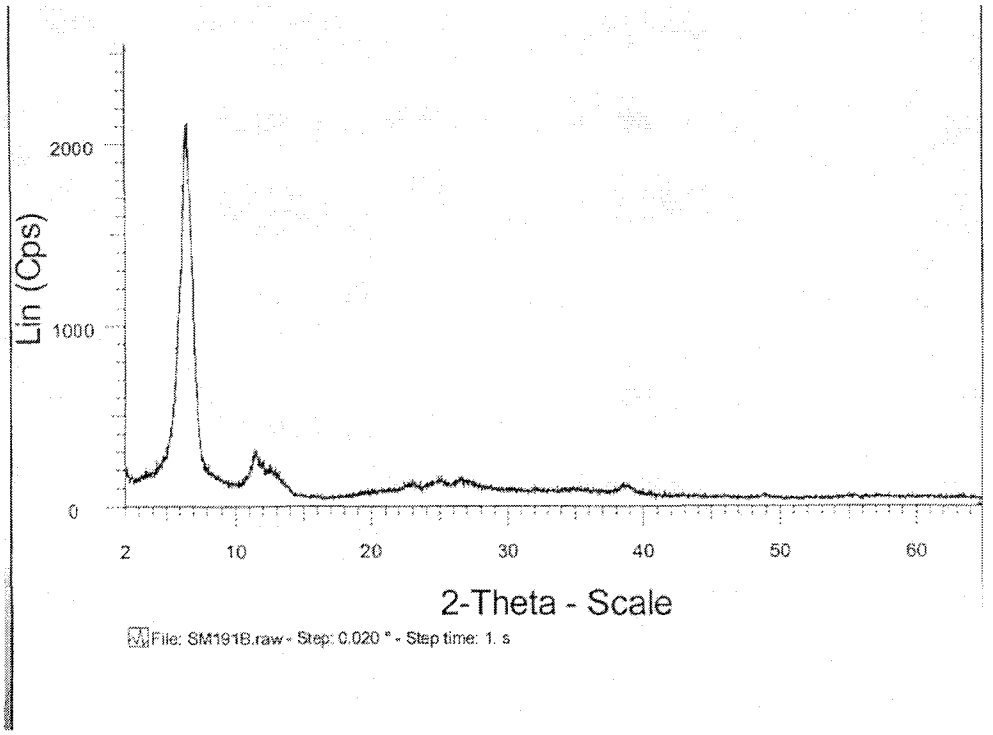

Figure 3.20. XRD of MoO_3/POMOE intercalate

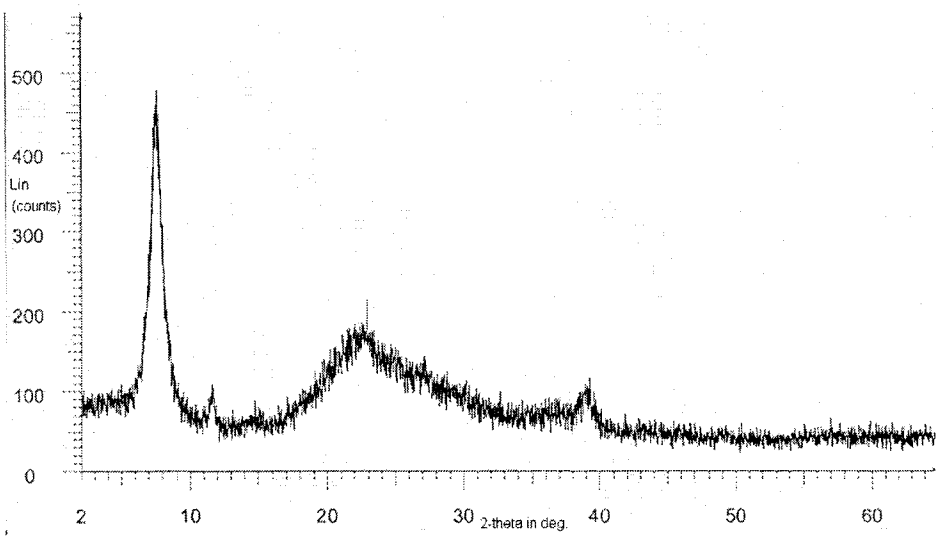

Figure 3.21. XRD of MoO_3/POEGO intercalate

3.5.4. Elemental and Thermogravimetric Analysis

The results of elemental analyses of Li_xMoO_3, POMOE/MoO_3 and POEGO/MoO_3 are summarized in the Table 3.

Table 3. Elemental Analysis of polymer-$LiMoO_3$ phase and lithiated MoO_3

Composite of $LiMoO_3$ with	Results%						
	C	H	N	O	S	Li	Mo
POMOE	9.89					1.25	45.9
POEGO	3.55					0.19	9.64
Elemental Analysis for $LiMoO_3$ in %							
	C	H	N	O	S	Li	Mo
						2.67	60.60

Using the data for the lithiated MoO_3 bronze, the stoichiometry of the material was found to be $Li_{0.6}MoO_3$.

Thermogravimetric analysis (TGA) was performed on a Mettler Toledo Star System using a heating rate of 10^0C/min under nitrogen and air. This technique was used to determine the thermal stability of the intercalates, and the composition of the materials were determined by using information obtained from the TGA and elemental analyses.

The thermogram under air for the nanomaterial, POMOE/MoO_3 shows a gradual weight loss up to 300^0C. The initial weight loss (3.47%) up to 100^0C is due to the evaporation of co-intercalated water molecules. The amount of weight loss from 96.50% to 74.34% was due to the elimination of POMOE from the gallery space of MoO_3. The stoichiometry of the intercalates can be represented by the general formula,

$$Li_x(H_2O)_y(Polymer)_z\,MoO_3$$

From elemental analyses the lithium and molybdenum contents of the nanocomposite were determined. Using the information from TGA and elemental analyses the composition of the nanocomposite was determined to be

$$Li_{0.38}(H_2O)_{0.38}(POMOE)_{1.03}\,MoO_3$$

The thermogram for the intercalate, POEGO/MoO_3 under air showed a gradual weight loss from room temperature to 275^0C. The loss of weight (1.5%) up to 100^0C was due to the evaporation of co-intercalated water molecules. The amount of weight loss from 96.50% to 90.12% was assigned to the elimination of POEGO from the gallery space of MoO_3. From elemental analyses the lithium and molybdenum content of the nanocomposite were determined. Using the

information from TGA and elemental analyses, the composition of the nanocomposite was determined to be

$$Li_{0.027}(H_2O)_{0.13}(POEGO)_{0.20}MoO_3$$

It is evident that all POMOE and a very small amount of POEGO used in the reactions entered the layered host of MoO_3. The ratio of lithium ions to molybdenum in $Li_{0.6}MoO_3$ was 0.6 and this value dropped to 0.38 and 0.027 after inclusion of POMOE and POEGO, respectively. This is reasonable because of the fact that some Li^+ ions were washed out as LiOH.

From the composition of the intercalates, it was observed that as the value of x (loading of intercalated lithium) in the nanocomposite decreased, the loading of co-intercalated water, y, and z (loading of POMOE/POEGO) also decreased. The decrease in the value of y with a concomittant decrease in the value of x supports the reaction between reduced MoO_3^{x-} and water molecules resulting in LiOH, which was washed out.

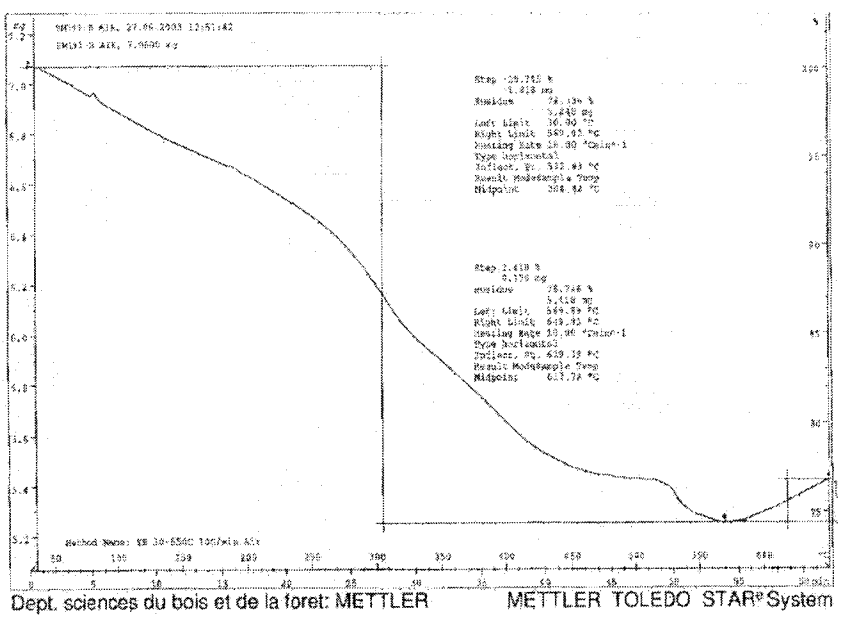

Figure 3.22. TGA of POMOE/ MoO_3 intercalate under air

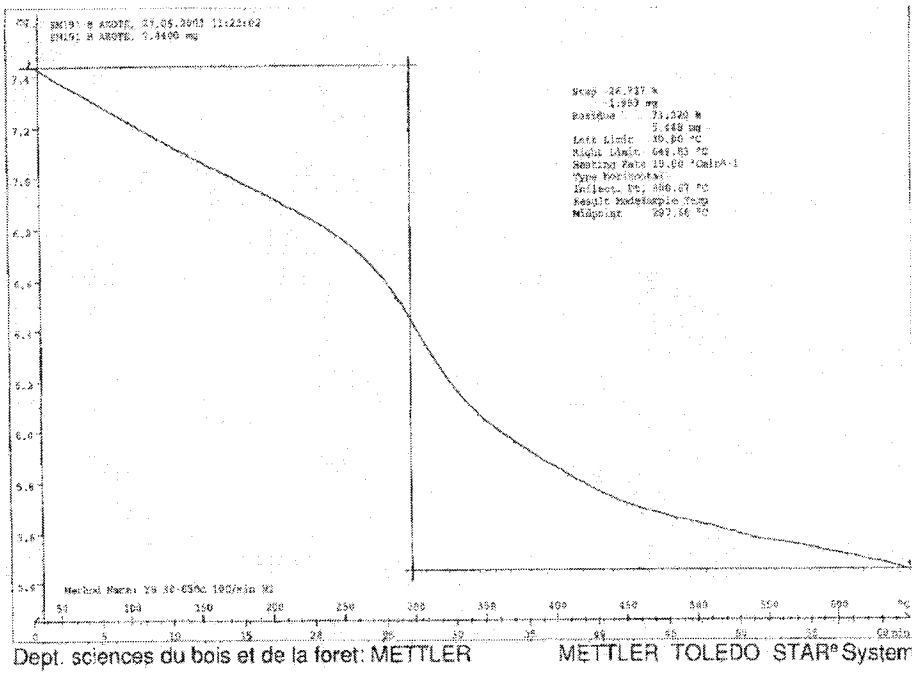

Figure 3.23. TGA of POMOE/ MoO_3 intercalate under nitrogen

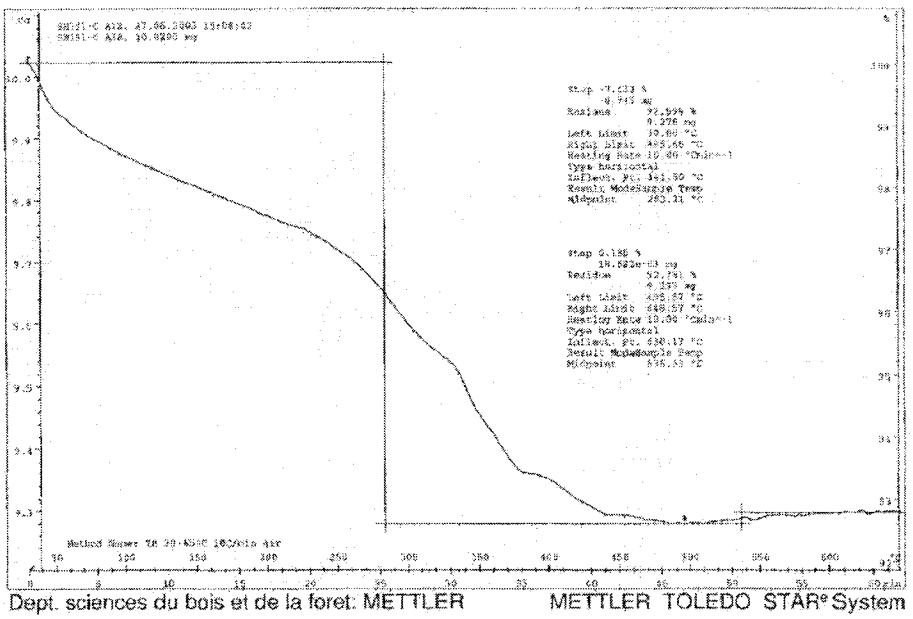

Figure 3.24. TGA of POEGO/ MoO_3 intercalate under air

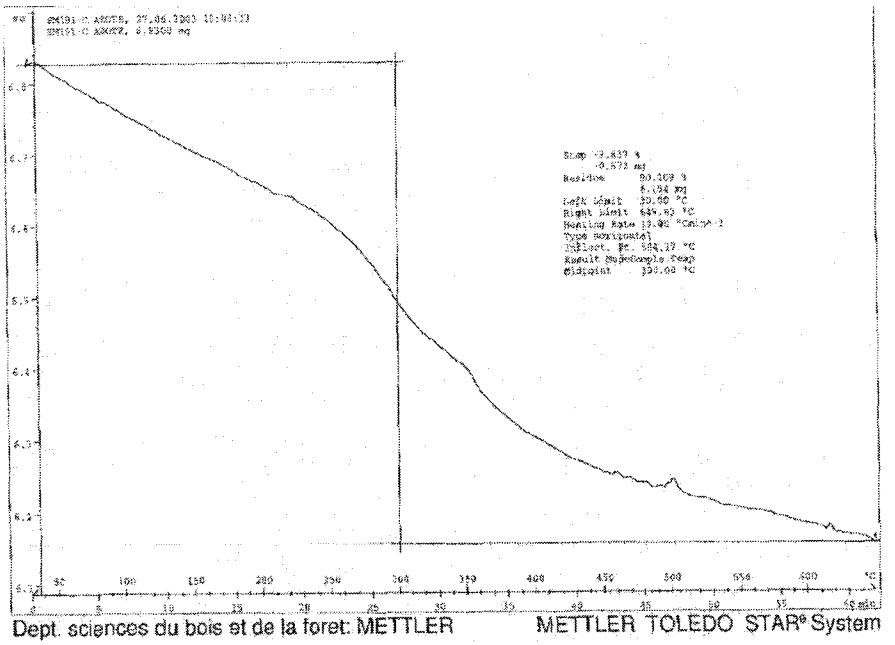

Figure 3.25. TGA of POEGO/ MoO_3 intercalate under air

3.6. POMOE/Li_xSnS_2 Intercalate

3.6.1. Reaction

The lithiated tin disulfide phase prepared by the redox reaction of SnS_2 with n-BuLi is described by Equation 3.5.

$$SnS_2 + x\,C_4H_9^-Li^+ \longrightarrow Li_x^+SnS_2^{x-} + {}^1/_2\,x\,C_8H_{18} \qquad (3.5)$$

where, the tin disulfide plates were reduced, gaining electrons from the oxidized $C_4H_9^-$. To counterbalance the negative charge on the reduced SnS_2 plates, Li^+ ions migrated into the gallery space of SnS_2.

The Li_xSnS_2 phase was partially exfoliated forming distorted layers of SnS_2 upon reaction with water with the aid of sonication.

$$LiSnS_2 + H_2O \longrightarrow \left(SnS_2\right)_{\substack{\text{partially}\\ \text{separated layers}}} + LiOH + H_2 \qquad (3.6)$$

The hydrogen that was formed pushed the layered sheets of SnS_2 apart providing a more spacious environment for partial accommodation of the polymer guests. The proposed mechanism for the inclusion of polymer guest species (POMOE/POEGO) has been shown in Figure 3.26.

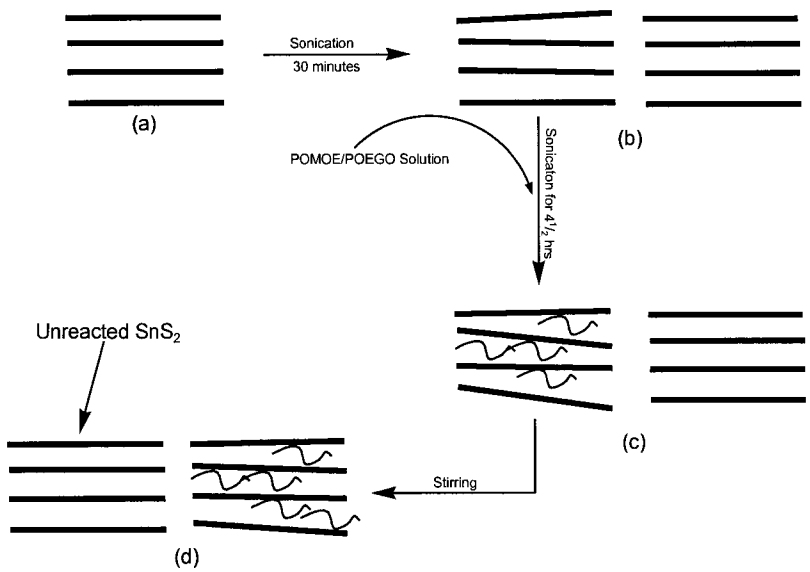

Figure 3.26. Partial intercalation of POMOE/POEGO in the lithiated phase of SnS_2 (a) virgin $LiSnS_2$ (b) very weak distortion of the SnS_2 layers (c) partial inclusion of the guest molecule with a bit more distortion of the SnS_2 layers (d) restacking of the SnS_2 sheets

It can be assumed that the following reactions took place in order to partially accommodate the polymer guest species.

$$\left(SnS_2\right)_{\substack{\text{partially}\\\text{separated layers}}} + x\,POMOE \longrightarrow \left(POMOE\right)_y SnS_2 + (x-y)\,POMOE \qquad (3.7)$$

$$\left(SnS_2\right)_{\substack{\text{partially}\\\text{separated layers}}} + x'\,POEGO \longrightarrow \left(POEGO\right)_z SnS_2 + (x'-z)\,POEGO \qquad (3.8)$$

where, y = loading of POMOE (partial intercalation), z = loading of POEGO (partial intercalation) and x, x/ > y, z. For simplicity, we may assume that x and x/ are the loadings for POMOE and POEGO, respectively, if the intercalation were complete.

3.6.2. Powder X-ray Diffraction

The XRD of the samples as cast thin films was run on a silicon substrate. The 00/ reflections confirmed the layered structure of the intercalates (POMOE/SnS_2 or POEGO/SnS_2) and pristine SnS_2. Thus, POMOE or POEGO was partially intercalated in SnS_2. The d-spacing of POMOE/SnS_2 and POEGO/SnS_2 were found to be 13.41 Å and 13.66 Å, respectively. The corresponding interlayer expansions were estimated to be 6.17 Å and 6.42 Å with respect to the pristine SnS_2 having a d-spacing value of 7.24 Å. Therefore, it can be assumed that a single layer of POMOE or POEGO partially entered into the SnS_2 layer host as shown in Figure 3.27.

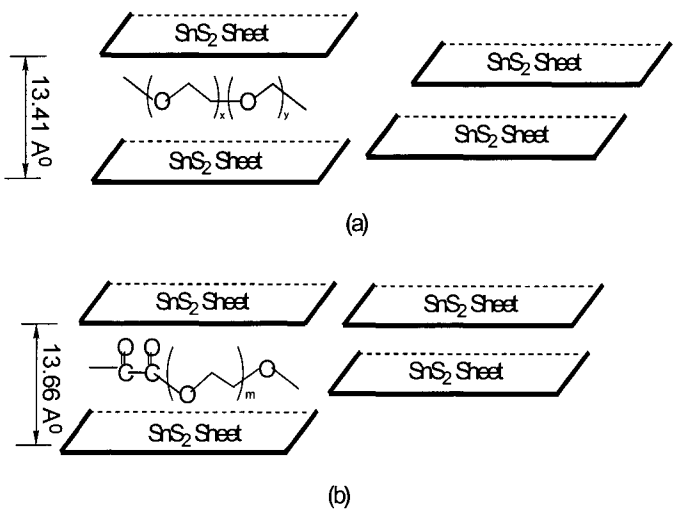

Figure 3.27. Schematic illustration of the proposed structure of (a) (POMOE)/SnS_2 intercalate (b) (POEGO)/ SnS_2 intercalate

The crystallite sizes of the nanocomposites were estimated from their powder X-ray diffraction pattern, using the Scherrer equation (Equation 2.10). The average crystallite size of pristine SnS_2, POMOE/SnS_2 and POEGO/SnS_2 were estimated to be 80 Å, 20 Å and 26 Å, respectively. The reduction in size upon intercalation could be due to improper restacking of the exfoliated SnS_2 layers compared to the pristine SnS_2.

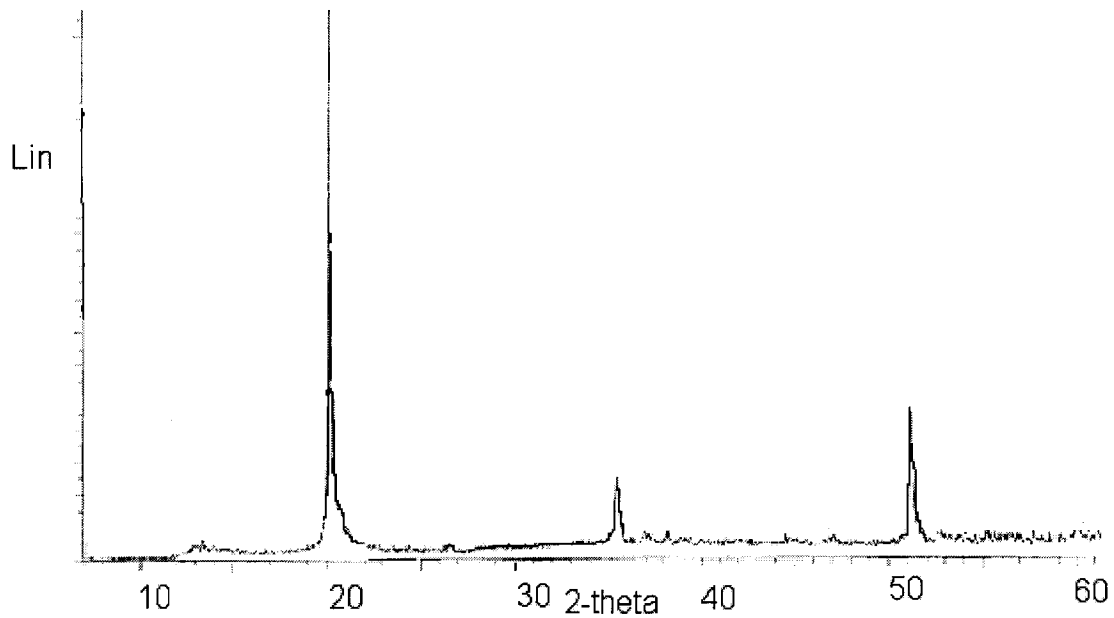

Figure 3.28. XRD of restacked SnS_2

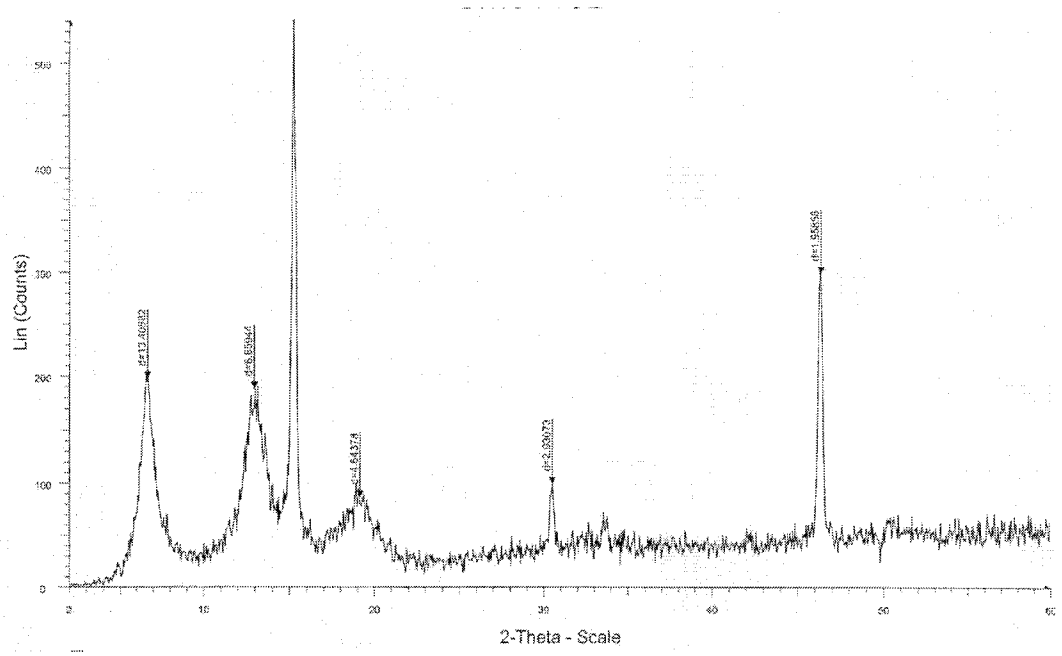

Figure 3.29. XRD of POMOE/SnS_2 intercalate (optimum condition)

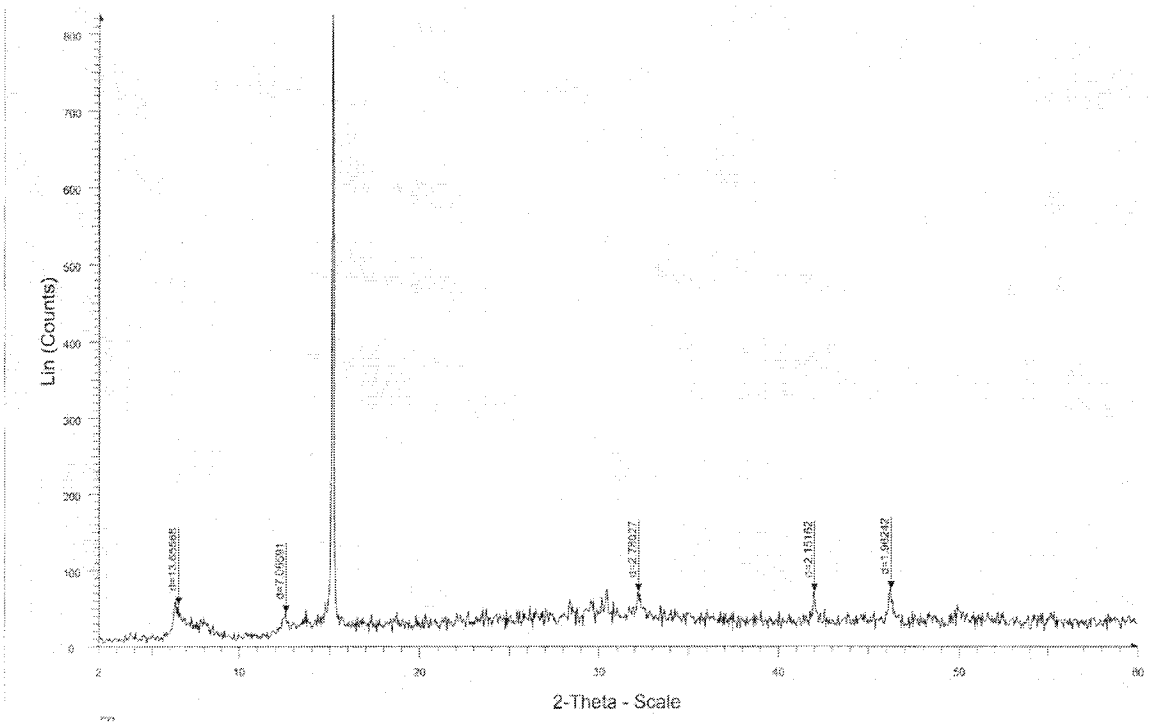

Figure 3.30. XRD of POMOE/SnS_2 intercalate (intercalation in progress)

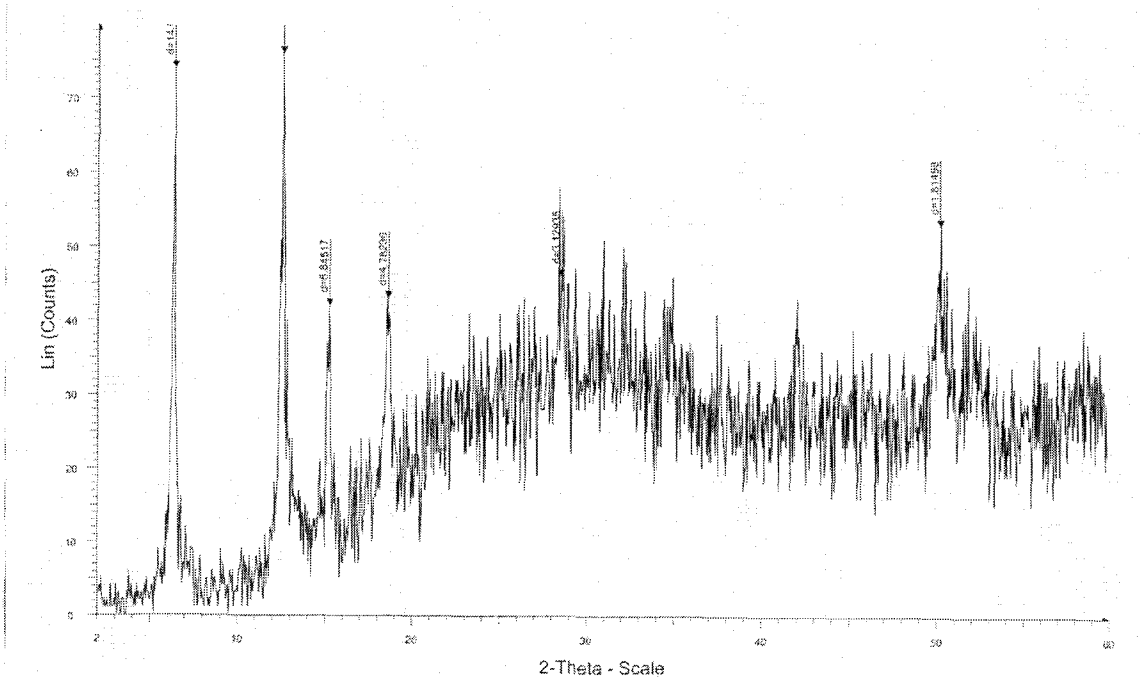

Figure 3.31. XRD of POEGO/SnS_2 intercalate (optimum condition)

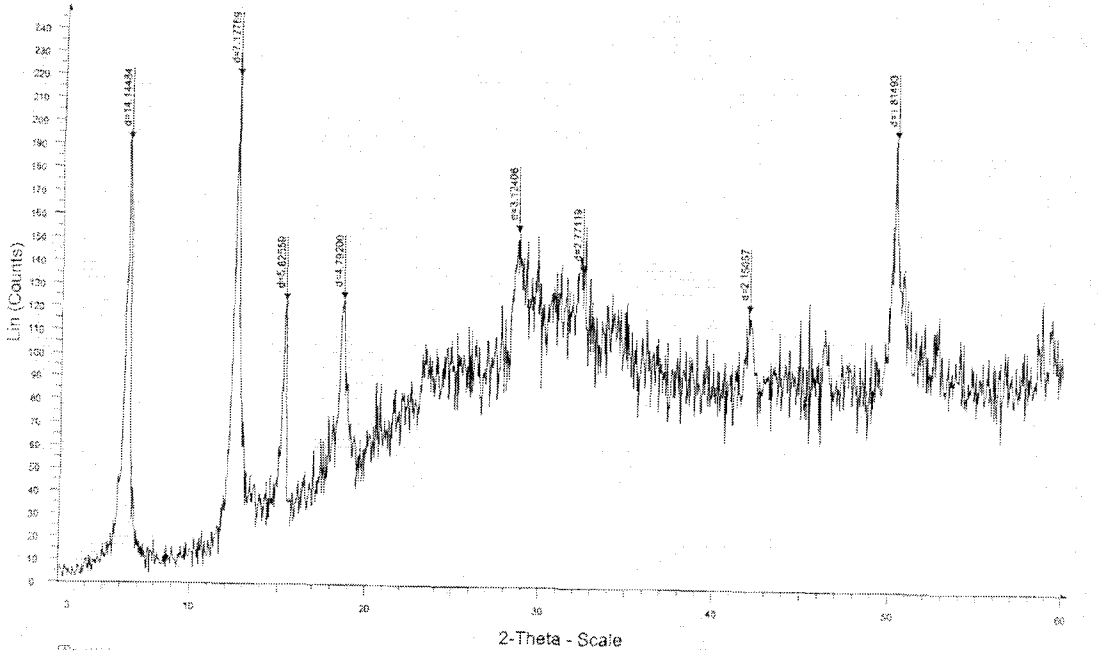

Figure 3.32. XRD of POEGO/SnS_2 intercalate (stirring for 47 days)

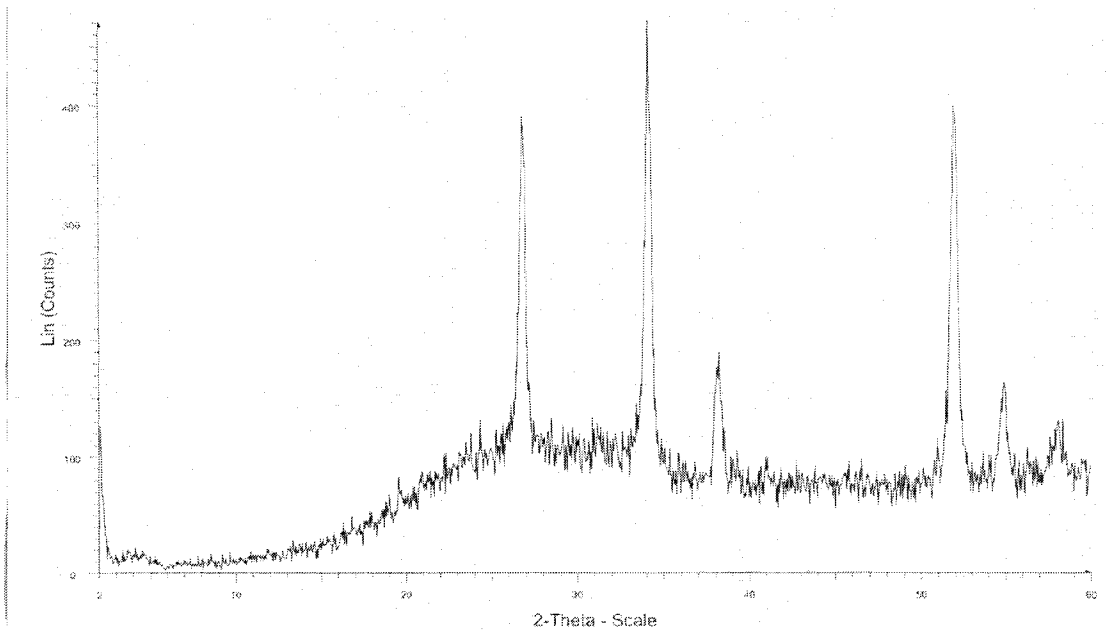

Figure 3.33. XRD of POEGO/SnS_2 (SnO_2) intercalate after heating upto 1000^0C

3.6.3. Thermogravlmetric Analysis

POMOE/SnS_2 was analyzed by TGA in air. The thermogram showed that there was an initial weight loss of 6.12 wt% of the intercalate up to 144^0C, which can be assigned to the loss of co-intercalated water molecules. The second step showing a gradual weight loss of 24.43% up to 550^0C, is due to the disappearance of POMOE. There was a slight weight gain of 2.84 wt% at 650^0C. This gain of weight can be assigned to the oxidation of co-intercalated lithium ions present in the system. Beyond this point, there was a weight loss of 5.69 wt% because of the formation of SnO_2 phase as confirmed by XRD. From the above data the proposed stoichiometry of the intercalate was determined to be $(H_2O)_{0.9}$ $(POMOE)_{0.15}SnS_2$.

Similarly, the thermogram of POEGO/SnS_2 showed a change in weight of 3.71wt% by 124^{0}C due to the evaporation of co-intercalated water. For simplicity, the next three steps of weight loss (8.37wt%, 10.80wt% and 6.87wt%) can be assigned to the loss of POEGO. The final weight loss (3.53wt%) could be due to the reaction between SnS_2 and oxygen to form SnO_2. The formation of SnO_2 was confirmed by XRD on the POEGO/SnS_2 system after performing TGA in air up to 1000^{0}C (Figure 3.33). From these information, the stoichiometry of the intercalate can be written as $(H_2O)_{0.5}$ $(POEGO)_{0.14}SnS_2$.

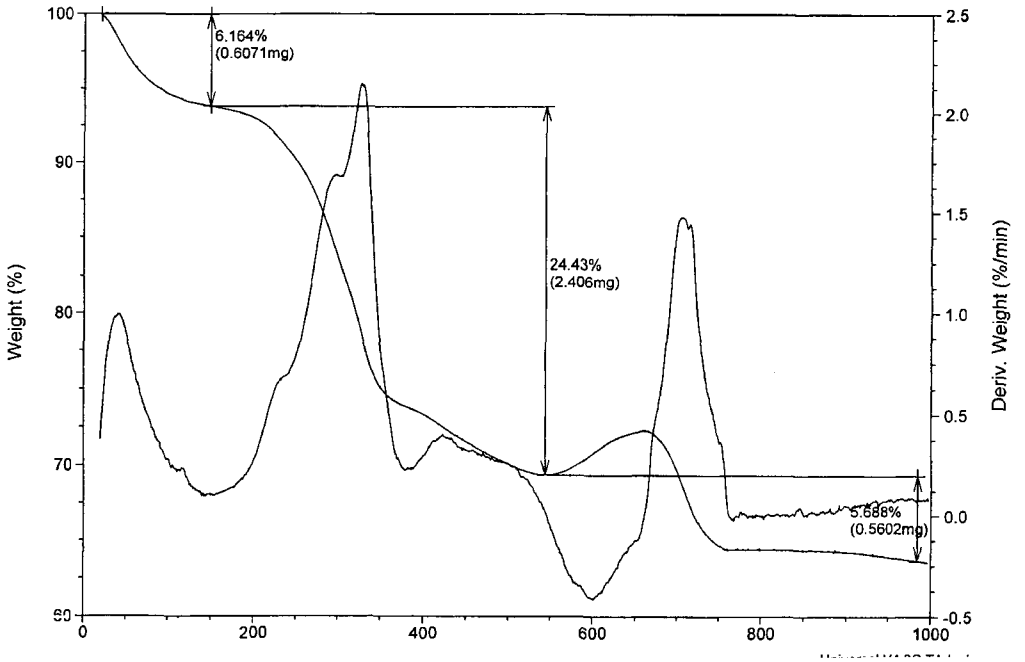

Figure 3.34.TGA of POMOE/SnS_2 intercalate

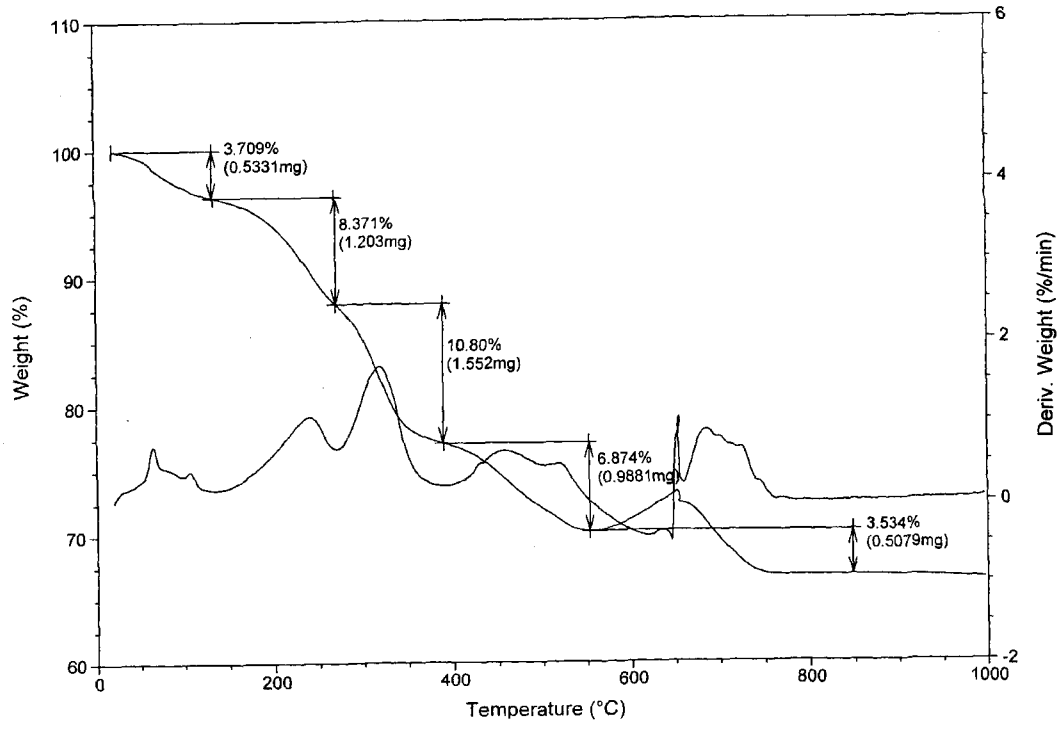

Figure 3.35. TGA of POEGO/SnS_2

3.7. Attempts to Obtain Complete Intercalation

To solve the issue of partial intercalation of POMOE and POEGO in SnS_2, several strategies were followed, which are summarized below.

3.7.1. Period of Sonication and Molar Ratio

Sonication helps in the homogeneous mixing and sometimes exfoliation of a layered host suspended in a suitable liquid medium. The effect of sonication period on the intercalation reaction was investigated. Keeping other parameters constant, the polymer/SnS_2 suspension was sonicated for 30 minutes and the reaction mixture was stirred for 3 days. This resulted in a very small amount of POMOE entering the gallery space of SnS_2 and no intercalation of POEGO was observed. Following the same procedure except sonicating the reaction mixture

for another 4½ hours after addition of the polymer, resulted in partial intercalation of POMOE and POEGO, and this is probably the *optimum condition* for the intercalation reaction (Sections 2.13, 2.14). It was observed that neither longer period of sonication nor stirring could result in any significant improvement of the intercalation. This was examined by continuing the sonication period up to 7 hours and stirring period for 47 days, and no further improvement in the intercalation results were found (Figure 3.31 and 3.32). In addition, the reactions were carried out using different polymer/SnS_2 ratios of 0.5, 1.5, 2.0. 2.5, 3.0 and 5.0 and following the same procedures as described in sections 2.13 and 2.14. Almost identical results were observed. Instead of using water as the dispersion medium, other polar solvents were used. These included dry MeOH, dry EtOH, MeOH/H_2O mixture (1:1 v/v) and EtOH/H_2O mixture (1:1 v/v). The reactions were carried out under aerobic and nitrogen conditions. Even with these various changes in the synthetic procedure, there were no further improvement in the intercalation results.

3.7.2. Intercalation of POMOE/POEGO in $LiSnS_2$ at Lower pH

Intercalation of the polymer (POMOE/POEGO) was examined using the successful procedure for POMOE/GO system (section 2.16). This attempt was unsuccessful for the intercalation of the polymers in SnS_2.

The partial intercalation of POMOE or POEGO in SnS_2 is not well understood. However, there might be two reasons for the partial intercalation. First, $LiSnS_2$ does not exfoliate completely using any of the abovementioned conditions. The incomplete exfoliation of $LiSnS_2$ in water has been confirmed by

XRD (Figure 3.28). In this case, the 00*l* reflections from $H_2O/LiSnS_2$ were slightly broader, but most of the SnS_2 remained unreacted. On the other hand, 00*l* reflections from MoO_3/H_2O showed very wide peaks (Figure 3.19), meaning that exfoliation of the system was complete. Second, there might be significant or complete exfoliation of the $LiSnS_2$ at some stage allowing the guest species to be encapsulated into the van der Waals gap of the host; but the bonding force between the layered sheets and the polymer is too weak that the system becomes unstable under some degree of external pressure. While thin films of the intercalates showed partial intercalation due to the presence of 00*l* reflections, the powdered form of the same films showed almost no intercalation (weak 00*l* reflections) . This might be because of the fact that the polymer species entering the layered host (SnS_2) could easily slip out under pressure even during the drying process. However, the former case i.e. the incomplete exfoliation of $LiSnS_2$ might be the main cause of partial intercalation.

3.8. POMOE/Graphite Oxide Intercalate

Oxidation of graphite to graphite oxide was successful as shown by XRD since the 00*l* reflections graphite (Figure 3.37) shifted to lower 2-theta values after formation of graphite oxide (Figure 3.38). The intercalation of POMOE into GO layered host was complete.

3.8.1. Powder X-ray diffraction

The XRD of the intercalate, $POMOE_x(H_2O)_yGO$, was run as a thin film on a silicon substrate. The interlayer spacing of the nanocomposite is 9.33 Å. The increase in interlayer spacing value from that of pristine GO (d-spacing, 8.35 Å) supports the formation of a new phase.

It was determined by TGA that virgin GO contains a layer of intercalated water molecules. Assuming the size of a water molecule to be 3.5 Å, the d-spacing value of GO without any water would be 4.85 Å. Since, the d-spacing value of POMOE/GO was found to be 9.33 Å, the net interlayer expansion of the GO sheets can be estimated as 4.48 Å. It can therefore be proposed that a single layer of POMOE was intercalated in between the van der Waals space of the GO sheets as shown in Figure 3.36.

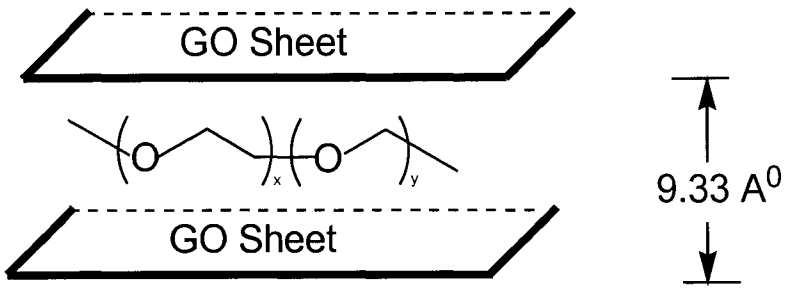

Figure 3.36. Schematic illustration of the proposed structure of $(POMOE)_xGO$

The average crystallite size of the intercalate was estimated from its X-ray diffraction pattern by using the Scherrer equation. The crystallite size of pristine GO used in the reaction was calculated to be 88 Å, and the crystallite size of the intercalate was estimated to be 50 Å. A reduction in crystallite size by almost 2 fold is an indication of non-identical re-stacking of the layered host after exfoliation, which is characteristic of most intercalated nanocomposites prepared through the exfoliation/restacking technique.

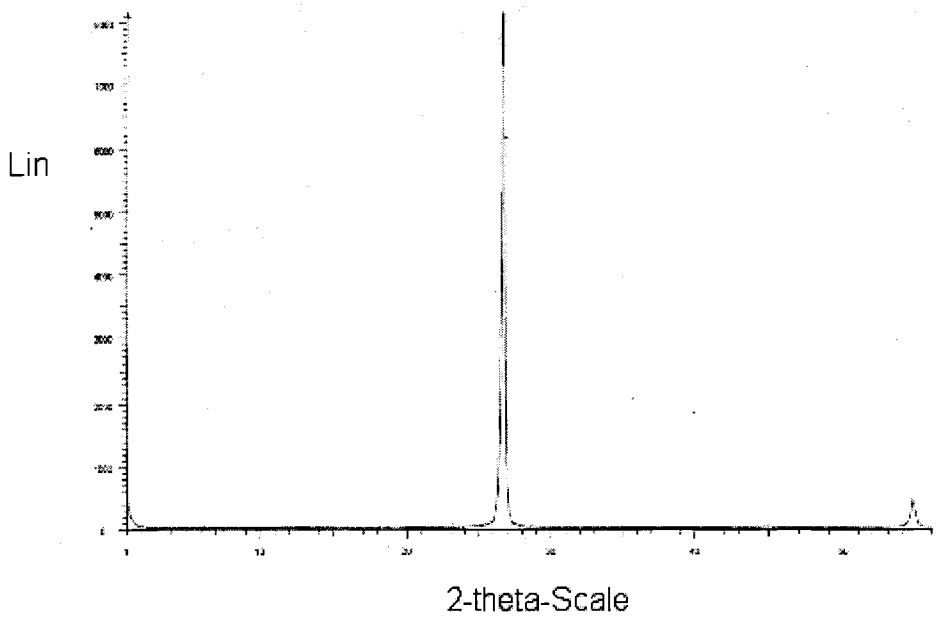

Figure 3.37. XRD of Graphite

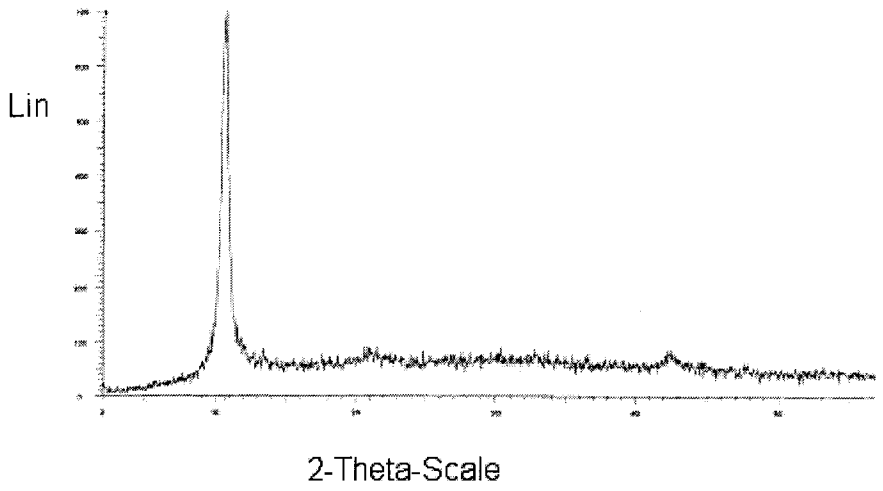

Figure 3.38. XRD of Graphite Oxide (GO)

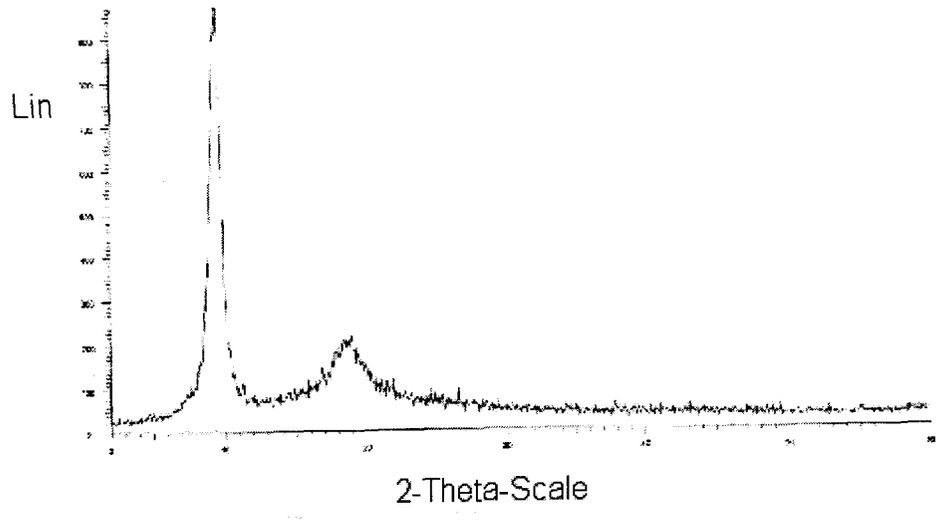

Figure 3.39. XRD of POMOE/GO intercalate

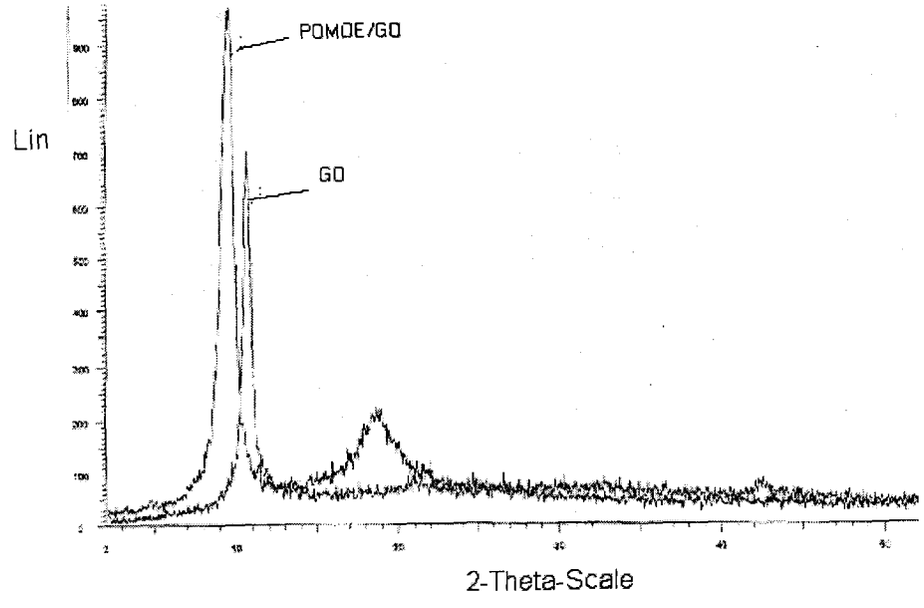

Figure 3.40. XRD of GO and POMOE/GO intercalate

3.8.2. Thermogravimetric Analysis (TGA)

To examine the thermal stability and composition of the intercalate (POMOE/GO), TGA was done by heating the sample up to 400^{0}C at a heating rate of 10^{0}C per minute in air. From the thermogram of the material, a weight loss of 5.16% was observed up to a temperature of 100^{0}C, which is due to the evaporation of co-intercalated water molecules. In the second decomposition step, a considerable amount of weight loss (55.26%) was observed up to 350^{0}C due to the elimination of POMOE.

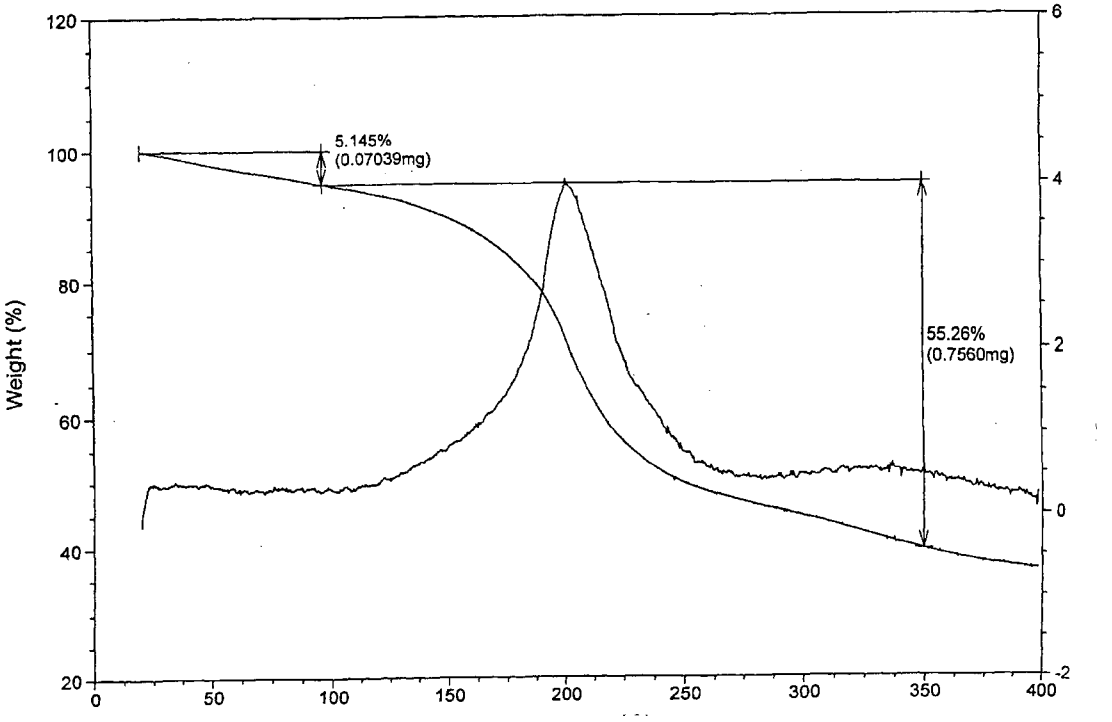

Figure 3.41. TGA of POMOE/GO

The rest of the material (GO) was approaching graphite (carbon) up to 400^{0}C, which was confirmed by XRD. From the thermogram, the composition of

the nanomaterial was estimated to be $(H_2O)_{0.9}(POMOE)_{0.39}GO$. This means that there are 0.39 moles of the repeat unit of POMOE per unit mole of GO.

Conclusion

The project was focused on the synthesis and characterization of polymer ionics, conductive polymers and intercalated nanocomposite materials, which can potentially be used as plastic electrolytes for solid-state rechargeable batteries. The route for the preparation of MEEP has been simplified. At the laboratory level, the synthesis of MEEP by this method takes only a day or two with higher yield. This has been achieved by synthesizing PDCP using a low temperature method that avoids the cross-linking problem associated with the high temperature ring opening polymerization of hexatrichlorocyclophosphazene. In addition, the sodium alkoxide solution was prepared by using NaH instead of sodium metal, which saves a considerable amount of time since the reaction rate for the prior case is faster. This may potentially attract researchers interested in in the chemistry of MEEP. A new substituted polymer of PDCP with PANI was synthesized and characterized. Surprisingly, this material was found to be soluble in water at or above 50^0C with the aid of sonication. This solubility property of the polymer could be further investigated in the future.

Three layered hosts namely, MoO_3, SnS_2 and graphite oxide (GO) were chosen for the intercalation of polar and amorphous polymers such as POMOE and POEGO by using exfoliation/restacking properties of the layered hosts. In aqueous medium, lithiated MoO_3 exfoliated completely and restacked with a bilayer of POMOE and POEGO. Similarly, in aqueous acidic medium, GO exfoliated completely and restacked with a single layer of POMOE as the guest

species. On the other hand, the lithiated SnS_2 layered system in water behaved differently, where partial exfoliation was only possible leading to partial insertion of POMOE and POEGO. Interestingly, all the final synthesized materials are air stable at ambient temperature.

This project leaves a lot of interesting research topics besides MEEP. The partial intercalation property of layered $LiSnS_2$ remains ambiguous. This could be either due to incomplete exfoliation of the layered host or slippage of guest species during restacking.

The synthesized new polymer, Poly[(diPANI)phosphazene] is amorphous as shown by XRD. This is one of the most desirable properties of polymer electrolytes and may be an interesting research area to pursue.

References

1. Whittingham, M.S.; Intercalation Chemistry: An Introduction, *Academic Press, Inc.*1982, 1

2. Besenhard, J.O.; Heydecke, E.W.; Fritz, H.P.; Foag, A. *Solid State Ionics* 8 (1983) 61

3. Johnson, J.W.; Jacobson, A. J.; Rich, S.M.; Brody, J.F. *J. Am. Chem. Soc.* 103 (1981), 5246

4. Guliants, V.V.; Benziger, J.B.; Sundaresan, S. *Chem. Mater.* 6 (1994) 353

5. Sienko, M.J.; Plane, R.A. *Chemistry, Principle and Application,* McGraw-Hill, Inc. New York 1979

6. Schöllhorn, R. Kuhlmann, R.; Besenhard, J.O.; *Mater. Res. Bull.* 83 (1976) 11

7. Bissessur R. Heising, J.; Hirpo, W.; Kanatzidis, M. *Chem. Mater.* 8 (1996) 318

8. Bissessur, R.; Gallant, D.; Brüning, R. *Solid State Ionics* 158 (2003) 205

9. Bissessur, R.; Gallant, D.; Brüning, R. *J. Mater. Sci. Lett.* 22 (2003) 429

10. Bissessur, R.; Wagner, B.D. *J. Mater. Sci.* 39 (2004) 119

11. Bissessur, R.; Haines, R.I.; Brüning, R. *J. Mater. Chem.* 3 (2003), 44

12. Bissessur, R.; Haines, R.I.; Hutching, D.R., Brüning, R. *Chem. Commun.* (2001), 1598

13.Scrosati, B. *Application of Electroactive Polymers,* Chapman & Hall 1993, 1

14. Chabagno, J.P., Duclot, M.J., *Makromol. Chem. Rapid Commun*. 1 (1980), 595

15. R. Spindler, D.F. Shriver, *Macromolecules* 21 (1988), 648

16. Keith J. Laidler; John H. Meiser, *Physical Chemistry*, The Benjamin/Cummings Publishing Co. Inc., 1982, 872

17. Liu,Y.J.; Degroot,D.C.; Schindler,J.I; Kannewurf,C.R.; Kanatzidis, M.G. *Chem. Mater. 3 (1991) 992*

18. Louis, E.J.; MacDiamid, A.G.; Chiang, C.K.; Heeger, A.J. *J. Chem. Soc., Chem. Commun.* (1977) 578

19. Lars Kihlborg, *Arkiv för Band* 21 (1963), 357

20. Hoang-Van, C.; Zegaoui, O. *Applied Catalysis A: general* 130 (1995) 89

21. Kambe, T.; Tsuboi, S.; Nagao,N.; Nogami, Y.; Oshima, K. *Physica. E* 18(2003) 196

22. Kihlborg L., *Arkiv* 21 (1963) 357

23. Magneli A., *Acta Cryst.* 6 (1953) 495

24. Bursill L.A., *Acta Cryst.* 6 (1972) 187

25. Nazar, L.F., Yin, X.T.; Zinkweg, D; Zhang Z; Liblong S. *Mater Res. Soc. Symp. Proc.,* (1991) 210

26. Balakumar. S., H.C. Zeng, *J. Cryst .Growth*, 194 (1998) 195

27. Nazar, L.F.; Zhang, Z.; Zinkweg D. *J. Chem. Soc.*, (1992), 114

28. Nazar, L.F.; Wu, H.; Power, W.P. *J. Mater. Chem.* 5 (1995), 1985

29. Oriakhi, C.O.; Lerner, M.M. *J. Chem. Mater.* 8 (1996), 2016

30. Tagaya, K. ; Kadokawa, A.J.; Chiba, k. *J. Chem. Mater.* 4 (1994), 551

31. Wang,L.; Schindler,J.; Kannewurf,C.R.; Kanatzidis, M.G. *J. Mater. Chem.* 7 (1997), 1277

32. Price, L.S.; Ivan, P.P.; Amanda, M.E. H.; Robin, J.H.C.; Thomas, G.H.; Kieran, C.M. *Chem. Mater.* 11 (1999) 1792

33. Radot, M. *Rev. Phys. Appl.* 18 (1977) 345

34. Ortiz, A.; Alonso, J.C.; Garcia, M.; Toriz, *J. Semicond. Sci. Technol.* 11 (1996) 243

35. Nair, P.K.; Nair, M.Y.S.; Fernandez, A.; Ocampo, M. *J. Phys. D. Appl. Phys.* 22 (1989) 829

36. Nair, M.T.S.; Nair, P.K. *Phys. D. J. Semicond. Sci. Technol.* 6 (1991) 132

37. Nazar, L.F.; Goward, G.; Leroux, F.; Duncan, M.; Huang, H.; Kerr, T.; Gaubicher, J. *Int. J. Inorg. Mater.* 3 (2001) 191

38. Morales, J.; Santos, J.; Barrado, J.R.R.; Espinós, J.P.; González-Elipe, A.R. *J. Solid State Chem.* 150 (2000) 391

39. Ollivier, P.J.; Kovtyukhova, N.I.; Keller, S.W.; Mallouk, T.E. *Chem. Commun.* 8 (1998) 1563

40. Tamás, S.; Szeri, A.; Dékány, I. *Carbon* (2005) 153

41. He, HY; Klinowski, J.; Forster, M.; Lerif, A.. *Chem. Phys. Lett.* 287 (1998), 53

42. Matsuo, Y.; Tahara,, K.; Sugie, Y. *Carbon 34* (1996), 672

43. Kovtyukhova, N.I.; Patricia, J. O.; Martin, B.R.; Mallouk, T.E.; Chizhik, S.A.; Buzaneva, E.V.; Gorchinskiy, A.D. *Chem. Mater.* 11 (1999) 771

44. Matsuo, Y.; Hatase, K.; Sugie, Y. *Chem. Mater.* 10 (1998), 2266

45. Matsuo, Y.; Tahara, K.; Sugie, Y. *Carbon* 35 (1997) 113

46. Liu, P.; Gong, K. *Carbon* 37 (1999) 701

47. Zheng, G.; Wu, J.; Wang, W.; Pan, C. *Carbon* 42 (2004) 2839

48. Christain, V.; Nicholas, D.; Booth, C. *Brit. Polym. J.* 20 (1988) 289

49. Wu Xu; Belieres, J.P.; Angell, C. A. *Chem. Mater.* 13(2001) 575

50. Lemmon, J. P. ; Wu,J.; Oriakhi,.C; Larner, M. M. *Electrochim. Acta* 40 (1995) 2245

51. Lagadic, I.; Leaustic, A.; Clement, R. *J. Chem. Soc. Chem. Commun.* (1992) 1396

52. Ruiz-Hitzky, E.; Aranda, P.; Casal, B. *J. Mater. Chem.* 2 (1992) 581

53. Ruiz-Hitzky, E.; Aranda, P. *Adv. Mater.* 2 (1990) 545

54. Liu, Y.J.; Degroot, D.C.; Schindler, J.L.; Kannewurf, C.R.; Kanatzidis, M. G. *Chem. Mater.* 3 (1991) 992

55. Bissessur,R.; Gallant,D; Brüning,R. *Mater. Chem. Phys.*82 (2003) 316

56. Stocks, H.N. *J. Am. Chem. Soc.* 19(1897), 782

57. Allcock, H.R.; Kugel, R.L. *J. Am. Chem. Soc.* 87(1965) 4216

58. Allcock, H.R.; Reeves, S.D.; Nelson, J.M.; Crane, C.A. *Macromolecules* 30 (1997), 2213

59. Wang, B.; Rivard, E.; Manners, I. *Inorg. Chem.* 41(2000), 1690

60. Peng, W.; Tan, K.L.; Zhang, F.; Kang, E,T.; Neoh, K.G. *Chem. Mater.* 13 (2001) 581

61. MacDiarmid, A.G.; Chang, J.C.; Richter, A.F.; Somasiri, N.L.D.; Epstein, A.J. "Polyaniline Synthesis and Characterization", *L. Alckcer (ed.) Conducting Polymers, D.Riedel Publishing Co.* 1987, 105

62. Zheng, W.Y.; Levon, K.; Laakso, J.; Österholm, J.E. *Macromolecules* 27(1994) 7754

63. Liu, P.; Gong, K.; Xiao, P.; Xiao, M. *J. Mater. Chem.* 10 (2000) 933

64. Allcock, H.R.; Reeves, S.D.; Chang, Y.; Lee, S.C.; Kim, K.T.; Kim, C. *Macromolecules* 34 (2001), 269

65. Allcock, H.R.; Crane, C.A.; Morrissey, C.T.; Nelson, J.M.; Reeves, S.D.; Honeyman C.H. Manners, I. *Macromolecules* 29 (2001), 7740

66. Chen-Yang, Y.W.; Hwang, J.J.; Huang, A.Y. *Macromolecules* 33 (2000) 1237

67. Bissessur, R.; DeGroot, D.C.; Kanatzidis, M.G.; Schindler, J.L.; Kannewurf, C.R. *J. Chem. Soc. Chem. Commun.* 1993, 68768. Ke, S.; Ying, M.; Ya-an, C.; Zhao-hui, C. *Chem. Mater.*13 (2001) 250

68. Ke, S.; Ying, M.; Ya-an, C.; Zhao-hui, C. *Chem. Mater.*13 (2001) 250